BBA - Molecular Basis of Disease 1871 (2025) 167767

Contents lists available at ScienceDirect

BBA - Molecular Basis of Disease

journal homepage: www.elsevier.com/locate/bbadis

Red blood cell proteomic profiling in mild and severe obstructive sleep apnea patients before and after positive airway pressure treatment

Cristina Valentim-Coelho [a,b,*], Joana Saraiva [a,b], Hugo Osório [c,d,e], Marília Antunes [f], Fátima Vaz [a,b], Sofia Neves [a,b], Paula Pinto [g,h], Cristina Bárbara [g,h], Deborah Penque [a,b,**]

[a] Laboratório de Proteómica, Departamento de Genética Humana, Instituto Nacional de Saúde Dr. Ricardo Jorge – INSA, 1649-016 Lisboa, Portugal
[b] Centro de Toxicogenómica e Saúde Humana (ToxOmics), Comprehensive Health Research Center (CHRC), Universidade Nova de Lisboa, 1150-082 Lisboa, Portugal
[c] Instituto de Investigação e Inovação em Saúde – i3S, Universidade do Porto, 4200-135 Porto, Portugal
[d] Instituto de Patologia e Imunologia Molecular da Universidade do Porto – Ipatimup, 4200-135 Porto, Portugal
[e] Departamento de Patologia, Faculdade de Medicina, Universidade do Porto, 4200-319 Porto, Portugal
[f] Centro de Estatística e Aplicações da Universidade de Lisboa e Departamento de Estatística e Investigação Operacional, Faculdade de Ciências, Universidade de Lisboa, 1749-016 Lisboa, Portugal
[g] Serviço de Pneumologia, Centro Hospitalar Lisboa Norte – CHLN, 1649-035 Lisboa, Portugal
[h] Instituto de Saúde Ambiental – ISAMB, Faculdade de Medicina, Universidade de Lisboa, 1649-026 Lisboa, Portugal

ARTICLE INFO

Keywords:
Obstructive sleep apnea (OSA) severity
Positive airway pressure (PAP)
Glycolysis
Pentose phosphate pathway (PPP)
Proteasome system
Red blood cells

ABSTRACT

Obstructive Sleep Apnea (OSA) is characterized by recurrent-episodes of apneas/hypopneas during sleep, leading to recurrent intermittent-hypoxia and sleep fragmentation. Non-treated OSA can result in cardiometabolic diseases.

In this study, we applied a shotgun-proteomics strategy to deeper investigate the red blood cell-(RBC) homeostasis regulation in the context of OSA-severity and their response to six months of positive airway pressure (PAP)-treatment. RBC-samples from patients with Mild/Severe-OSA before/after-PAP treatment and patients as

Abbreviations: 2,3-BPG, 2,3-bisphosphoglycerate; AHI, Apnea-hypopnea index; ALDOA, Fructose-bisphosphate aldolase A; ALDOC, Fructose-bisphosphate aldolase C; ANK1, Ankyrin-1; ATP, Adenosine triphosphate; BMI, Body mass index; BPGM, Bisphosphoglycerate mutase; CA2, Carbonic anhydrase 2; CO_2, Carbon dioxide; CUL3, Cullin-3; DAVID, Database for Annotation, Visualization and Integrated Discovery; DCUN1D1, DCN1-like protein 1; DDB1, DNA damage-binding protein 1; DHAP, Dihydroxyacetone phosphate; EMP, Embden-Meyerhof-Parnas; ENO1, Alpha-enolase; EPB42, Erythrocyte membrane protein band 4.2; EPW, Epworth sleepiness scale; ESI, Electrospray ionization; FDR, False discovery rate; G6PD, Glucose-6-phosphate 1-dehydrogenase; GAPDH, Glyceraldehyde-3-phosphate dehydrogenase; GGCT, Gamma-glutamylcyclotransferase; GLC, Glucose; GLO1, Lactoylglutathione lyase; GLUT4, Glucose transporter, type 4; GOT1, Aspartate aminotransaminase; GSH, Glutathione synthesis; GSS, Glutathione synthetase; Hb, Hemoglobin; HbA1C, Hemoglobin glycated; HCD, Higher-energy collisional dissociation; HOMA-IR, Model assessment of insulin resistance; kDa, Kilo Dalton; LC, Liquid chromatography; LDHA, L-lactate dehydrogenase A chain; LDHB, L-lactate dehydrogenase B chain; LFQ, Label-free quantitation; LM, Linear model; LMM, Linear mixed model; MAPK, Mitogen-activated protein kinase; MCV, Mean corpuscular volume; MDH1, Malate dehydrogenase; MG, Methylglyoxal; MS, Mass spectrometry; MW, Molecular weight; NAD^+, Nicotinamide adenine dinucleotide; NADH, Reduced nicotinamide adenine dinucleotide; NADPH, Nicotinamide adenine dinucleotide phosphate; NAE1, NEDD8-activating enzyme E1 regulatory subunit; NEDD8-MDP1, Nedd8; Non-oxiPPP, Non-oxidative PPP; O_2, Oxygen; ODI, Oxygen desaturation index; OSA, Obstructive Sleep Apnea; Oxi-PPP, Oxidative PPP; PA max, Maxim Arterial Pressure (Systolic); PA min, Minim Arterial Pressure (Diastolic); PAP, Positive airway pressure; PEP, Phosphoenolpyruvate; PGK1, Phosphoglycerate kinase 1; PKLR, Pyruvate kinase; PPP, Pentose phosphate pathway; PSG, Polysomnography; PSM, Peptide spectrum matching; PSMB6, Proteasome subunit beta type-6; PSMB7, Proteasome subunit beta type-7; PSMD2, 26S proteasome non-ATP regulatory subunit 2; PSMD7, 26S proteasome non-ATPase regulatory subunit 7; PSME1, Activator complex subunit 1; PSME2, Activator complex subunit 2; PSMF1, Proteasome inhibitor PI31 subunit; RBC, Red blood cell(s); RDI, Respiratory disturbance index; RDW, Red cell distribution width; RPIA, Ribose-5-phosphate isomerase; SD, Standard deviation; SLC4A1, Band 3 anion transport protein; SUMO, Small ubiquitin-like modifier; SUMO2, Small ubiquitin-related modifier 2; t0, Before PAP treatment; t6, After six months of PAP treatment; TALDO1, Transaldolase; TCR, T cell receptor; TPI, Triosephosphate isomerase; UBA1, Ubiquitin-like modifier-activating enzyme 1; UBADC1, Ubiquitin-associated domain-containing protein 1; UBE2K, Ubiquitin-conjugating enzyme E2 K; UBE2N, Ubiquitin-conjugating enzyme E2 N; UBE2V1, Ubiquitin-conjugating enzyme E2 variant 1; UBLs, Ubiquitin-like proteins; UHPLC, Ultra-high-performance liquid chromatography; UPS, Ubiquitin-like Proteasome System; USP14, Ubiquitin carboxyl-terminal hydrolase 14; USP15, Ubiquitin carboxyl-terminal hydrolase 15; WB, Western blot.

* Corresponding author.
** Correspondence to: D. Penque, Laboratório de Proteómica, Departamento de Genética Humana, Instituto Nacional de Saúde Dr. Ricardo Jorge – INSA, 1649-016 Lisboa, Portugal.
E-mail addresses: cristina.valentim@insa.min-saude.pt (C. Valentim-Coelho), deborah.penque@insa.min-saude.pt (D. Penque).

https://doi.org/10.1016/j.bbadis.2025.167767
Received 1 July 2024; Received in revised form 5 January 2025; Accepted 25 February 2025
Available online 4 March 2025

simple-snoring controls were selected. The mass-spectrometry raw-data was analysed by MaxQuant for protein identification/quantification followed by statistical Linear Models-(LM) and Linear Mixed Models-(LMM) to investigate OSA-severity effect and interaction with PAP, respectively. The functional/biological network analysis were performed by DAVID-platform.

The results indicated that key-enzymes of the *Embden-Meyerhof-Parnas* (EMP)-glycolysis and pentose phosphate pathway-(PPP) were differentially changed in Severe-OSA, suggesting that the O_2-dependent metabolic flux through EMP and PPP maybe compromised in these cells due to severe intermittent hypoxia/reoxygenation-induced oxidative-stress events in these patients. The Rapoport-Luebering-glycolytic shunt showed a significant downregulation across OSA-severity maybe to increase hemoglobin-O_2 affinity to adapt to O_2 low availability in the lung, although EMP-glycolysis showed decreased only in Severe-OSA.

Proteins of the immunoproteasome were upregulated in Severe-OSA maybe to respond to severe oxidative-stress. In Mild-OSA, proteins related to the ubiquitination/neddylation-(Ub/Ned)-dependent proteasome system were upregulated.

After PAP, proteins of Glycolysis and Ub/Ned-dependent proteasome system showed reactivated in Severe-OSA. In Mild-OSA, PAP induced upregulation of immunoproteasome proteins, suggesting that this treatment may increase oxidative-stress in these patients. Once validated these proteins maybe candidate biomarkers for OSA or OSA-therapy response.

1. Introduction

Obstructive sleep apnea (OSA) is the most prevalent sleep respiratory disorder, but the majority remains undiagnosed and thus untreated. Nearly 1 billion adults aged 30–69 years worldwide may be affected by OSA [1–3]. OSA is characterized by recurrent nocturnal episodes of upper airway hypopnea/apnea for at least 10 s and in a number of 5 episodes or more per hour of sleep causing intermittent hypoxia and sleep fragmentation associated with arousals, leading to cellular homeostasis perturbation. OSA is classified as mild, moderate, or severe based on the number of apneic events per hour [2,4,5].

Non-treated OSA can result in cognitive and behavioural deficits, cardiovascular and metabolic disorders, such as hypertension, stroke, diabetes mellitus and even cancer. These comorbidities are associated with increased early morbidity and mortality in patients with OSA compared with the general population of the same age group [2,4,6]. Integration of OSA screening into routine clinical care has therefore been strongly recommended for the prevention of OSA and its related outcomes. However, the gold standard for the diagnosis of OSA, the nocturnal laboratory-based polysomnography (PSG), is expensive, time consuming and not widely available. Portable home monitoring device is an alternative but not without costs being confirmation by PSG often necessary [2,5]. Positive airway pressure (PAP) has long been considered the first-line treatment for most patients with OSA because it is efficacious, cost-effective, and non-invasive, although side negative effects have also been reported, and not all patients benefit from it [2,7].

For all these reasons, a cost-efficient blood biomarker for OSA screening in a large population, the identification of individuals at risk of developing this pathology and, consequently, the complications associated with it, is needed, therefore allowing the prevention and control of OSA and OSA outcomes. The identification of biomarkers able to predict or monitor the effectiveness of PAP therapy will also advance OSA clinical care [2,8].

In addition to plasma, red blood cells (RBCs) can be a useful biological source for biomarker research in OSA. RBCs are the most abundant cells in the body (comprising over 80 %), acting as both transporter, deliverer and sensor of oxygen (O_2) [2,9]. RBCs also play noncanonical functions, including systemic antioxidant activity, control of blood rheology, erythrocrine function (i.e., by releasing bioactive molecules), as well as, a signaling mediator of the immune system [10–12]. Dysfunction in RBC homeostasis has been described as a potential source of systemic inflammation leading to metabolic and cardiovascular diseases such as those resulting from non-treated OSA [2].

By using traditional 2D gel-based proteomics, our group investigated for the first time the RBC proteome from OSA patients to better understand this pathology underlying mechanisms, while uncover potential biomarkers for OSA [2,13]. The results indicated that changes in RBC proteins/proteoforms associated with the biological process such as cell death, H_2O_2 catabolic/metabolic process, stress response, and protein oligomerization, involving redox regulators, might be compromising the RBC homeostasis in OSA. PAP treatment showed to restore the modulation of some of these proteins/proteoforms in patients [2,13].

In the present study, we applied a shotgun proteomics strategy to deeper investigate the RBC homeostasis regulation in the context of Mild and Severe clinical spectrum of OSA manifestation before and after six months of PAP therapy. The main findings indicated that the proteome associated with glycolysis energy metabolism, glutathione antioxidant defence and proteasome system regulating protein degradation/signaling mechanism are the main differentially modulated in OSA severity spectrum and response to PAP treatment.

2. Material and methods

2.1. Patients and samples

One hundred four consecutive male subjects with clinically suspected OSA syndrome were recruited under informed consent for blood biobanking collection, clinical and biochemical evaluation as we previously described [2,14]. Exclusion criteria were female gender (to avoid hormonal influence), shift workers, other sleep disorders and comorbidities (e.g., neuromuscular disease, heart failure, diabetes, neoplasia, acute disease) and previous PAP treatment.

Patients with suspected OSA were hospitalized overnight at the sleep laboratory for the polysomnography (PSG) study according to standard procedures. PAP therapy was prescribed for patients diagnosed with OSA (RDI $\geq$ 5/h) as we previously described [2,14]. Biochemical analyses were performed according to the hospital standard procedures, including 24 h urinary catecholamines, glycemic and lipidic profiles and complete hemogram at the baseline (t0, hospitalization day for PSG diagnosis) and after treatment (t6, after six months of PAP treatment). Venous blood samples were collected on the evening of the day of admission and the next day morning after overnight fasting into EDTA-coated polypropylene tubes for a biobank sample preparation as described in our previous studies [2,13–15]. Fasting morning blood samples were also collected from patients after six months of PAP treatment for biobanking as mentioned above.

From the biobank, only 'morning' RBC samples corresponding to subjects with primary snoring (RDI $\leq$ 5/h, $n = 23$), patients with Mild (RDI $\geq$ 5/h, but $\leq$15/h, $n = 16$) and Severe OSA (RDI $\geq$ 30/h, $n = 17$) before and after six months of PAP treatment, were selected for this shotgun proteomics study (Table 1).

The protocol of this project was approved by Ethics Committees of the Centro Hospitalar Lisboa Norte (CHLP), Hospital Santa Maria, Lisboa, Portugal (January 6, 2012) and Instituto Nacional de Saúde Doutor

Table 1
Cohort demographic data & polysomnographic and clinical parameters.

Data/parameters	Snorers	All OSA	Mild	Severe
Subjets (100 % male) (n)	23	33	16	17
Age (years)	44.8 (9.6)	46.9 (7.5)	46.1 (8.5)	47.6 (6.6)
Current Smoking (n)	9	5	2	3
Observational features				
Morning arterial pressure (mmHg)#	134.9 (17.2)/83.4 (11.9)	131.4 (17.6)/84.4 (11.7)	129.1 (19.3)/79.9 (10.3)	133.5 (16.1)/88.5 (11.7)
BMI (kg/m^2)	27.2 (3.2)	30.3 (3.1)**	29.2 (2.9)*	31.3 (2.9)**$^{\Delta}$
Abdominal perimeter (cm)	97.5 (7.7)	105.8 (8.5)**	102.8 (7.2)*	108.8 (8.8)**$^{\Delta}$
Comorbidities				
Hypertension (n)	6	22	9	13
Respiratory diseases (n)	0	0	0	0
Dyslipidemia (n)	9	18	7	11
Diabetes (n)	0	0	0	0
Polysomnographic parameters				
RDI (events/h)	2.7 (1.4)	32.5 (26.2)**	9.2 (2.4)**	54.4 (17.7)**$^{\Delta\Delta}$
ODI (events/h)	2.2 (3.3)	27.5 (26.0)**	6.8 (2.7)**	47.0 (22.7)**$^{\Delta\Delta}$
Sleep efficiency (%)	78.1 (12.2)	75.2 (16.7)	77.8 (15.9)	72.6 (17.5)
Arousal index (%)	14.2 (6.0)	29.3 (17.8)**	17.5 (6.3)	40.5 (17.9)**$^{\Delta\Delta}$
Minimum arterial saturation (%)	89.3 (2.9)	82.8 (6.2)**	85.6 (3.8)*	80.1 (6.9)**$^{\Delta}$

PAP treatment							
		All OSA		Mild		Severe	
Before/after PAP	–	t0	t6	t0	t6	t0	t6
EPW Score	9.5 (4.8)	10.9 (5.0)	6.3 (4.6)**	11.81 (4.4)	7.0 (7.8)**	10.1 (5.5)	5.7 (4.5)*
PAP record							
Number of days without use	–	–	44.1 (49.0)	–	41.6 (40.1)	–	46.5 (57.3)
Total of recording days	–	–	271.7 (121.4)	–	249.8 (91.8)	–	292.2 (143.6)
Residual AHI	–	–	1.7 (1.3)	–	1.8 (1.2)	–	1.7 (1.3)
Analytical parameters							
Glycemic profile							
Glucose (70–110 mg/dL)	92.9 (7.9)	96.2 (12.2)	94.5 (14.2)	92.6 (9.5)	91.1 (9.1)	99.5 (13.7)	97.7 (17.3)
Hb A1C (4–6 %)	5.5 (0.4)	5.6 (0.4)	5.6 (0.6)	5.5 (0.4)	5.5 (0.4)	5.8 (0.4)$^{\Delta}$	5.8 (0.8)
Insulin (3–25 mU/L)	12.4 (6.1)	16.9 (10.4)	25.8 (32.1)	10.6 (4.1)	11.2 (4.7)	22.8 (11.1)**$^{\Delta\Delta}$	39.6 (40.3)$^{\Delta\Delta}$
HOMA-IR (≥3.8)	2.9 (1.5)	4.1 (2.6)	6.4 (8.7)	2.4 (0.9)	2.5 (0.9)	5.7 (2.7)**$^{\Delta\Delta}$	10.1 (10.9)$^{\Delta\Delta}$
Lipid profile							
Cholesterol (<190 mg/dL)	190.3 (37.0)	189.2 (40.4)	184.0 (32.4)	189.7 (50.4)	184.2 (31.7)	188.7 (29.6)	183.9 (34.0)
Triglycerides (<150 mg/dL)	118.9 (62.9)	135.4 (64.8)	142.9 (85.0)	119.3 (55.0)	117.7 (49.8)	150.6 (71.1)*	166.5 (104.3)
Cardiovascular marker							
Homocysteine (3.7–13.9 μmol/L)	15.4 (3.8)	16.5 (6.9)	17.4 (5.7)	17.2 (9.6)	18.5 (7.6)	15.9 (2.7)	16.5 (3.1)
Urinary catecholamines							
Adrenalin (1.7–22.4 μg/24 h)	20.4 (17.7)	17.0 (12.0)	17.3 (9.7)	16.3 (14.2)	17.0 (7.4)	17.7 (9.8)	17.5 (11.7)*
Nor-adrenalin (12.1–85.5 μg/24 h)	64.0 (29.4)	70.1 (33.6)	56.7 (20.8)	65.3 (37.2)	57.5 (17.7)	74.6 (30.3)	56.0 (23.9)
Dopamine (0–498 μg/24 h)	375.5 (201.0)	345.2 (181.0)	320.6 (134.3)	339.7 (211.1)	311.7 (126.2)	350.3 (153.9)	329.0 (144.8)
Complete hemogram							
RBC (4.5–5.9 × 10^{12}/L)	5.1 (0.4)	5.2 (0.3)	5.0 (0.3)*	5.1 (0.3)	4.9 (0.3)*	5.2 (0.3)	5.1 (0.3)$^{\Delta}$
Hemoglobin (13–17.5 g/dL)	15.3 (0.8)	15.6 (1.0)	15.1 (0.9)**	15.2 (0.8)	14.9 (0.7)*	15.9 (1.1)$^{\Delta}$	15.3 (1.1)**
Hematocrit (40–50 %)	45.0 (2.1)	45.7 (3.0)	44.3 (2.8)*	44.8 (2.5)	43.2 (2.3)*	46.6 (3.2)	45.4 (2.8)*$^{\Delta}$
MCV (80–97 fl)	89.1 (5.6)	88.7 (3.9)	88.6 (3.5)	88.5 (3.9)	88.3 (2.9)	88.8 (4.0)	88.6 (4.0)
RDW (11.5–14.5)	13.5 (0.5)	13.5 (0.7)	13.6 (0.7)	13.2 (0.7)	13.5 (0.7)	13.8 (0.6)$^{\Delta}$	13.8 (0.6)
Platelets (150–450 × 10^3 μL)	232.2 (47.5)	224.4 (50.3)	205.7 (48.4)*	231.9 (55.6)	213.5 (54.7)*	217.4 (45.3)	198.5 (41.9)

Statistical significance: **p value < 0.001 and *p value < 0.05, comparing non-treated (t0) OSA (all/mild/severe) vs Snorers, or OSA (all/mild/severe) after (t6) vs before PAP treatment (t0); $^{\Delta\Delta}$p value < 0.001 and $^{\Delta}p$ value < 0.05, comparing Severe OSA vs Mild OSA before (t0) or after PAP (t6). #PA max/PA min.

Ricardo Jorge, Lisboa, Portugal (April 9, 2013). The project was registered at the Comissão Nacional de Proteção de Dados (CNPD) and all patients gave written informed consent (Table 1).

2.2. RBC sample preparation

In brief, RBCs samples were obtained after blood centrifugation for 10 min. at 1800 rpm at 4 °C, washed three times with PBS, discarding as much as possible the supernatant containing leukocytes and platelets, and the final pellet containing >99 % of RBCs were aliquoted for storage in a − 80 °C biobank until used. The selected samples were randomly pooled ($n = 3$ per group/condition) and lysed (1:6) with 5 mM sodium phosphate buffer pH 7.4 containing 100 mM of N-ethylmaleimide, a reagent that alkylates free sulfhydryl groups, and 1:100 cocktail of protease inhibitors (P8340, Sigma Aldrich, Darmstadt, Germany) for 10 min at 4 °C followed sonication in an ultrasonic bath during 1 min. After centrifugation at 25,000 ×*g* for 20 min, at 4 °C (Centrifuge 5417R, Eppendorf, Hamburg, Germany), the supernatants were recovered for hemoglobin (Hb) depletion using Hemovoid depletion columns (Biotech Support Group, Monmouth JCT, NJ, USA), according to the manufacture's protocol. The fractions obtained after depletion were concentrated and buffer-exchanged with 25 mM NH_4HCO_3 pH 8.4 by centrifugal filtration using 3 kDa Molecular Weight Cut-Offs (MWCO) 0.5 mL sample volume (Amicon Ultra-0.5, Millipore, Darmstadt, Germany) spin concentrators. The protein concentration was determined by a colorimetric assay (Pierce™ 660 nm Protein Assay Kit, Thermo Fisher Scientific, Waltham, MA, USA) according to the manufacturer's protocol. Samples were dried using a SpeedVac (Concentrator Plus, Eppendorf, Hamburg, Germany) and stored at −80 °C until use.

2.3. Peptide preparation: in-solution digestion

In dried Hb-depleted pooled samples, each containing 50 μg of protein, 90 μL 6 M urea was added, followed by sample reduction with 10 mM dithiothreitol (DTT) solution (in 200 mM NH_4HCO_3) and incubation for 1 h at 37 °C with shaking (300 rpm). The samples reduced were alkylated by adding 20 mM iodoacetamide (IAA) solution (in 200 mM NH_4HCO_3) and incubation proceeded for 30 min at room temperature, in the dark. The samples were diluted with 200 mM NH_4HCO_3 for a final concentration of 1 M urea and the trypsin was added in a 1:20 (enzyme: protein) ratio. The digestion took place overnight (no >16 h and with agitation at 300 rpm); then $CaCl_2$ was added (10 mM $CaCl_2$ - final concentration in sample), followed by chymotrypsin digestion at 1:20 (enzyme:protein) ratio and incubation at 37 °C, for 4 h–6 h with agitation (300 rpm). The digestion reaction was inhibited by acidification with 10 % formic acid final volume and after centrifugation at 232 ×*g* by 5 min (mixed well). Samples were dried in speed vacuum. The resulting peptides were cleaned using C18 spin columns (BioPureSPN™ Macro Desalting Columns, 35–350 μg maximum capacity, The Nest Group, USA) for salt removal and sample preparation for MS, according to the manufacturer's protocol.

2.4. Protein identification by shotgun proteomics

2.4.1. LC-MS/MS analysis

The peptides purified obtained were processed using a nano LC-MS/MS, composed by an Ultimate 3000 liquid chromatography system coupled to a Q-Exactive Hybrid Quadrupole-Orbitrap mass spectrometer (Thermo Scientific, Bremen, Germany). Samples were loaded onto a trapping cartridge (Acclaim PepMap C18 100 Å, 5 mm × 300 μm i.d., 160,454, Thermo Scientific, Bremen, Germany) in a mobile phase of 2 % ACN, 0.1 % FA at 10 μL/min. After 3 min loading, the trap column was switched in-line to a 50 cm by 75 μm inner diameter EASY-Spray column (ES803, PepMap RSLC, C18, 2 μm, Thermo Scientific, Bremen, Germany) at 250 nL/min. Separation was generated by mixing A: 0.1 % FA and B: 80 % ACN, with the following gradient: 5 min (2.5 % B to 10 % B), 120 min (10 % B to 30 % B), 20 min (30 % B to 50 % B), 5 min (50 % B to 99 % B), and 10 min (hold 99 % B). Subsequently, the column was equilibrated with 2.5 % B for 17 min. Data acquisition was controlled by Xcalibur 4.0 and Tune 2.9 software (Thermo Scientific, Bremen, Germany).

The mass spectrometer was operated in data-dependent (dd) positive acquisition mode alternating between a full scan (m/z 380–1580) and subsequent HCD MS/MS of the 10 most intense peaks from full scan (normalized collision energy of 27 %). Electrospray ionization (ESI) spray voltage was 1.9 kV. Global settings: use lock masses best (m/z 445.12003), lock mass injection Full MS, chrom. peak width (Full width at half maximum—FWHM) 15 s. Full scan settings: 70 k resolution (m/z 200), automatic gain control (AGC) target 3×10^6, maximum injection time 120 ms; dd settings: minimum AGC target 8×10^3, intensity threshold 7.3×10^4, charge exclusion: unassigned, 1, 8, >8, peptide match preferred, exclude isotopes on, dynamic exclusion 45 s. MS2 settings: microscans 1, resolution 35 k (m/z 200), AGC target 2×10^5, maximum injection time 110 ms, isolation window 2.0 m/z, isolation offset 0.0 m/z, dynamic first mass, and spectrum data type profile.

2.5. Protein identification and label-free quantification

Raw data corresponds to the three technical replicates from each pool. The raw data were analysed with Andromeda search engine within MaxQuant freeware software (version 1.5.8.3) [16], using a human protein sequence database from the UniProt Knowledgebase (UniProtKB) (February 4, 2022). The search was performed with Carbamidomethylation, Oxidation of Methionine and N-ethylmaleimide of cysteine as variable modifications. Trypsin/P and chymotrypsin were selected as proteases allowing up to two missed cleavages, and the peptide mass was limited to a maximum of 4600 Da. Mass search tolerances were 20 ppm and 0.5 Da for MS and MS/MS, respectively. Peptide spectrum matching (PSM), protein and site were both applied at 1 % false discovery rate (FDR). Label-free quantification with a minimum ratio count of 2 was used, where unique and razor peptides were employed for quantification. In general, parameters in MaxQuant have not been changed from their default values unless explicitly stated. The identified proteins are shown in Table S1 in Supplementary material.

The obtained MS results were processed by Perseus platform v2.0.7.0 for protein identification and label-free relative quantification [17]. Proteins identified with a high confidence MaxQuant-Andromeda score $\geq$ 40, at least one unique peptide and one MS/MS count among the different groups were selected for further statistical analysis. For that, protein LFQ intensity values were $\log_2$ transformed, and missing values imputed from a mean of intensities around the detection limit of the mass spectrometer.

2.6. Protein annotation and classification

Protein annotation properties were acquired using the Database for Annotation, Visualization and Integrated Discovery (DAVID) v2021 (Frederick National Laboratory, USA) [18]. This open-source tool retrieves a set of biological and functional information such as Gene Ontology (GO terms – subcellular location, molecular function and biological process) and analysis of biological pathways through Reactome platform with p value < 0.05. The Reactome pathways are shown in Fig. 3.

2.7. Statistical analysis

2.7.1. Clinical parameters

Descriptive analyses for clinical and analytical data were expressed as mean ± standard deviation (SD). Nonparametric tests (distribution free tests) were used to analyse ordinal data, to statistically compare two groups. Mann-Whitney test was employed to compare Snorers and OSA groups (all OSA t0, Mild t0 and Severe t0 conditions) and between OSA

severity groups for t0 and t6 (Mild and Severe). Wilcoxon test was used to evaluate the effect of (before/after) PAP treatment on the different OSA groups. The statistical analysis was performed using IBM SPSS Statistics 28 (Armonk, NY, USA) and the level of statistical significance set at 5 % (p value < 0.05).

2.7.2. Differential protein abundance analysis

Differences in protein abundance ($\log_2$ transformed) between pools of the control (Snorers) and OSA groups (Mild, Severe) before and after PAP treatment, were determined by simple linear regression. Fitting for each protein emulated the following model,

$$Protein\ Abundance \sim Group$$

in which, as demonstrated, Group was the predictor when comparing all OSA patients or patients with Mild or Severe OSA with Snorers.

Concomitantly, for differences in protein expression throughout time a linear mixed-effects model was applied, where a parameter accounting for the repeated measures of the pools, with the same individuals, measured at t0 and t6 was added, following one of the models:

$$Protein\ Abundance \sim Time + (1|ID_{Pool})$$

or

$$Protein\ Abundance \sim Group \times Time + (1|ID_{Pool})$$

Time alone was used as a predictor when comparing all OSA before and after PAP treatment; and Group, Time, and the interaction term Group × Time were the explanatory variables when comparing OSA severity groups (e.g., Mild, Severe) and PAP treatment effect.

Statistical analysis was performed in R version R-4.3.2, through the RStudio 2022.12.03 (Boston, MA, USA) workbench. For model's estimation lme4 package was used, and the p values for model fits were determined by Satterthwaite's degrees of freedom method, by the lmerTest package [19,20].

For additional group/time comparisons, in the former, group or time were used as a main effect, while in the latter, time, group and the interaction term time × group and or just time as predictors, in both models, the package emmeans was used to obtain estimated marginal means, and the contrasts and respective confidence intervals determined [21]. P value adjustment for multiple comparisons was executed through the Dunn–Šidák correction (control family-wise error rate). Representation of the contrast results was through forest plots, using the ggplot2 package [22,23]. Bars and Spaghetti graphs were used to plot the LM and LMM results, respectively. Additional packages included tidyverse and dplyr for data manipulation [24,25].

3. Results

3.1. Clinical presentation, biochemical, and metabolic characteristics

The significant results are summarized in Table 1. PSG parameters were significantly different between non-treated (t0) OSA patient's groups and the Snorer group (Mann-Whitney test p value < 0.001), as expected. The body mass index (BMI) and abdominal perimeter were increased in all non-treated (t0) OSA (Mann-Whitney test p value < 0.001), either with Mild OSA (Mann-Whitney test p value < 0.05), or Severe OSA (Mann-Whitney test p value < 0.001), when compared with Snorer controls. Insulin resistance, determined by homeostatic model assessment of insulin resistance (HOMA-IR), and the lipid profile for the triglycerides were significantly increased in Severe OSA t0 (Mann-Whitney test p value < 0.001) but not in patients with Mild OSA t0, compared with the control group. The hematological parameters, RBC and hemoglobin, displayed a significant increase, and the platelets a decrease in all non-treated OSA patients compared to Snorers (Mann-Whitney test p value < 0.05). In terms of severity, modulation of PSG parameters (Mann-Whitney test p value < 0.001), as well as BMI, abdominal perimeter, HbA1C, Insulin, HOMA-IR, RBC, hemoglobin and RDW (Mann-Whitney, p value < 0.05) was noted, showing higher levels in Severe OSA subjects when compared with Mild OSA subjects, at t0.

After six months (t6) of PAP treatment (compliance with mean usage >4 h night), patients reported a significant decrease in excessive daytime somnolence, as evaluated by the Epworth Sleepiness Scale (EPW) score; the hemogram data, although showing clinical normal reference values, revealed a slight but significant decrease in hemoglobin concentration and RBC, hematocrit and platelet counts after PAP treatment (Wilcoxon test, p value < 0.05).

There were no significant changes in glucose and lipid profile and cardiovascular marker after PAP treatment. However, in patients with Severe OSA at t6, an increase in urinary adrenalin catecholamine was discerned (Wilcoxon test, p value < 0.05).

3.2. Shotgun proteomics of OSA RBCs

In total, 1466 proteins were identified by shotgun proteomics on hemoglobin depleted RBCs samples, being 362 proteins identified with a high confidence MaxQuant-Andromeda score ≥ 40.

Fig. 1 displays the Venn diagrams with the distribution of the 362 identified proteins among the different groups/conditions, i.e., between Snorers and All OSA at t0 and t6 (Fig. 1, A) or between Snorers and patients with Mild OSA or Severe OSA at t0 and t6 time point (Fig. 1, B). The majority of these proteins were identified in all groups/conditions, being few proteins identified as unique to each group/condition or between the different groups.

3.3. Proteomics data analysis by LM and LMM statistical approaches

346 proteins identified with at least one unique peptide and one MS/MS count in all technical triplicate were quantified and statistically analysed across all sample groups/conditions. Proteomic data is shown in the Supplementary material Table S1. Protein normalized abundance values of each protein were fitted using simple regression (LM) and mixed-effects models (LMM). In the former, group was used as a main effect, while in the latter, time or time, group and the interaction term time × group as predictors.

Fig. 2 depicts the forest plots of the proteins shown to be significantly modulated among Snorer control and all OSA patient's group across the time points, t0 and t6. A total of 29 differentially expressed proteins were identified in all OSA patients (t0) compared with Snorers (LM p value < 0.05) (Fig. 2, A). OSA patients before (t0) and after six months of PAP treatment (t6) exhibited significant differential changes (LMM p value < 0.05) in 37 proteins (Fig. 2, B).

Compared with Snorer group, non-treated Mild OSA or Severe OSA (t0) presented 14 and 27 significant differentially expressed proteins (LM p value < 0.05), respectively (Fig. 2, C, D). Six months of PAP treatment induced significant changes (LMM p value < 0.05) in 22 and 11 proteins in Mild OSA and Severe OSA, respectively (Fig. 2, E, F). By comparing OSA patients in terms of disease severity, i.e., Severe OSA versus Mild OSA, before treatment (t0) or post-treatment (t6), a total of 47 and 21 differentially expressed proteins (LMM p value < 0.05) were identified, respectively (Fig. 2, G, H). The abundance of differentially expressed proteins ($\log_2$ transformed), the fold change ($\log_2$FC) and the values of corresponding adjusted p are shown in Table S2 in Supplementary material.

3.4. Reactome pathways

The differentially expressed proteins identified by the LM and LMM statistical approaches with p value < 0.1 were further analysed by the DAVID platform v2021 to retrieve the most significant Reactome pathways (p value < 0.05), taking into consideration the RBC activity and function.

Fig. 3 shows the obtained results displayed by Bubble Charts. In all

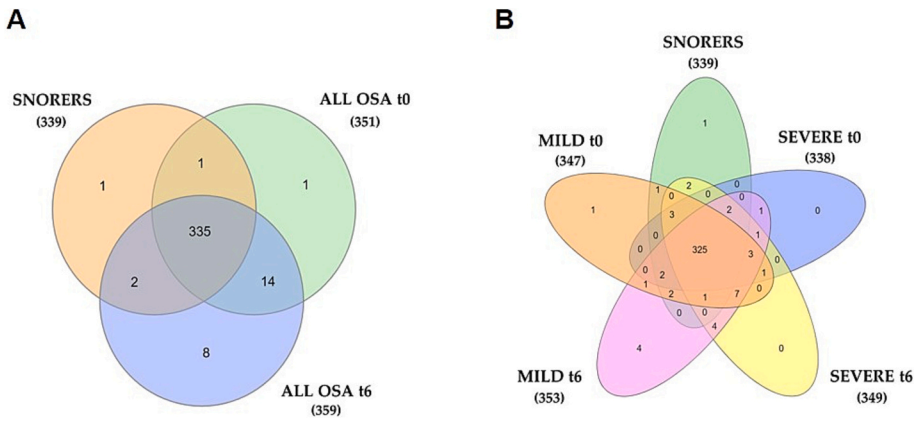

Fig. 1. Venn diagram analysis of proteins identified with MaxQuant-Andromeda high confidence score. (A) Venn diagram representing the overlap of identified proteins between Snorers and all OSA before (t0) and after six months of PAP treatment (t6). (B) Venn diagram representing the overlap of identified proteins between Snorers and Mild and Severe OSA subgroups before (t0) and after treatment (t6). MaxQuant-Andromeda high confidence score was established as ≥40.

OSA (t0), a total of 45 differentially expressed proteins showed to be associated with translocation of GLUT4 to the plasma membrane, negative regulation of MAPK pathway, deubiquitination, immune system and programmed cell death (Fig. 3, A). In response to PAP treatment, the 55 differentially expressed proteins identified in all OSA were involved with cellular response to chemical stress, alterations in immune system, signaling by interleukins, programmed cell death, ubiquitination and proteasome degradation, glutathione conjugation and pentose phosphate pathway (Fig. 3, B). In Mild t0 group, compared with Snorer, the 33 differentially expressed proteins were associated with cellular response to chemical stress, O_2/CO_2 exchange in erythrocytes, neutrophil degranulation, immune system, neddylation, ubiquitination and proteasome degradation and cellular response to hypoxia (Fig. 3, C). When compared with Snorer, Severe OSA group (t0) showed a greater number of significant differentially expressed proteins than Mild OSA group, 55 proteins with p value < 0.1. These proteins showed to be associated with pathways such as glucose metabolism, programmed cell death, glycolysis, neddylation, cellular response to stress and hypoxia, and deubiquitination (Fig. 3, D).

In response to PAP treatment, a total of 47 and 21 differentially expressed proteins with LMM p value < 0.1 were identified, respectively, in Mild OSA and Severe OSA. In Mild OSA, the differentially expressed proteins were associated with interleukins signaling, immune system, programmed cell death, glucose and pyruvate metabolism, ubiquitination and proteasome degradation (Fig. 3, E). In Severe OSA, these proteins were shown to be associated with cellular response to chemical stress, neddylation, T cell receptor (TCR) signaling, innate immune system and programmed cell death (Fig. 3, F).

By comparing Severe OSA t0 versus Mild OSA t0, 67 differentially expressed proteins were identified as related with cellular response to chemical stress and to hypoxia, O_2/CO_2 exchange in erythrocytes, glycolytic pathways as glucose metabolism, innate immune system, neddylation, programmed cell death, detoxification of reactive oxygen species and ubiquitination and proteasome degradation (Fig. 3, G). After PAP treatment (t6), the 25 differentially expressed proteins identified between Severe OSA and Mild OSA, showed to be associated with cellular response to chemical stress and to stimuli, membrane trafficking, diseases of metabolism, purine catabolism and neurodegenerative diseases (Fig. 3, H).

3.5. Proteins of glycolysis cycle and glutathione synthesis were differentially modulated in OSA severity and OSA severity response to PAP treatment

In an attempt to evaluate the Mild and Severe spectra of OSA severity and their response to PAP treatment, the RBC proteomics data were analysed by a linear regression analysis using $\log_2$ transformed LFQ protein intensity values as the response variable. The comparison of each OSA group (Mild and Severe) with the control (Snorers) was performed by a simple linear regression model (LM), while the comparison of Mild or Severe OSA response to PAP treatment, a linear mixed model (LMM) was employed to assess potential proteome differences between groups at t0, as well as the proteome variation through time (t0 vs t6), which could be attributed or associated with the treatment. *P* values were adjusted to control for the multiple testing problem through the application of the Dunn–Šidák correction with a 5 % significance level using the emmeans package in R.

Several proteins of both the *Embden-Meyerhof-Parnas* (EMP) pathway and pentose phosphate pathway (PPP) of glycolysis cycle, and proteins of glutathione (GSH) synthesis were identified differentially modulated according to OSA severity spectrum and their response to PAP treatment (Figs. S1 and 4).

In Severe OSA, the EMP glycolytic proteins such as the fructose-bisphosphate aldolase C (ALDOC) was significantly increased while pyruvate kinase (PKLR), l-lactate dehydrogenase A chain (LDHA) and l-lactate dehydrogenase B chain (LDHB) PKLR, LDHA and LDHB showed a significant decrease compared to Snorers (Fig. S1, A–D) (LM p value = 0.042, p value = 0.029, p value = 0.005 and p value = 0.012, respectively).

The bisphosphoglycerate mutase (BPGM), a central enzyme in the *Rapoport–Luebering* shunt of EMP glycolytic pathway, was significantly decreased in both Mild OSA (LM p value = 0.001) and Severe OSA (LM p value = 0.043) compared with Snorers (Fig. S1, E). The carbonic anhydrase 2 (CA2) was also found significantly decreased but only in Mild OSA (LM p value = 0.007) (Fig. S1, F).

In Severe OSA, the key regulator of the non-oxidative PPP (non-oxiPPP) arm involved in purine salvage reactions, the ribose-5-phosphate isomerase (RPIA), exhibited a significant increase compared to controls (LM p value = 0.028) (Fig. S2, G).

Two proteins associated with GSH synthesis, a key molecule in antioxidant defence, were also found differentially modulated in OSA severity. The gamma-glutamylcyclotransferase (GGCT) was decreased in Mild OSA (LM p value = 0.037), and the glutathione synthetase (GSS) increased in Severe OSA (LM p value = 0.009) (Fig. S1, H, I). The cytosolic aspartate aminotransaminase (GOT1), that also contributes to NADPH and reduced GSH generation, showed an increase only in Severe OSA compared with Snorers (LM p value = 0.004) (Fig. S2, J).

In response to PAP treatment, several proteins of Glycolytic and GSH synthesis pathways were also found differentially modulated and some of this modulation showed interaction with OSA severity condition.

The glycolytic enzymes, fructose-bisphosphate aldolase A (ALDOA) and ALDOC were higher in Severe OSA, compared with Mild OSA at t0

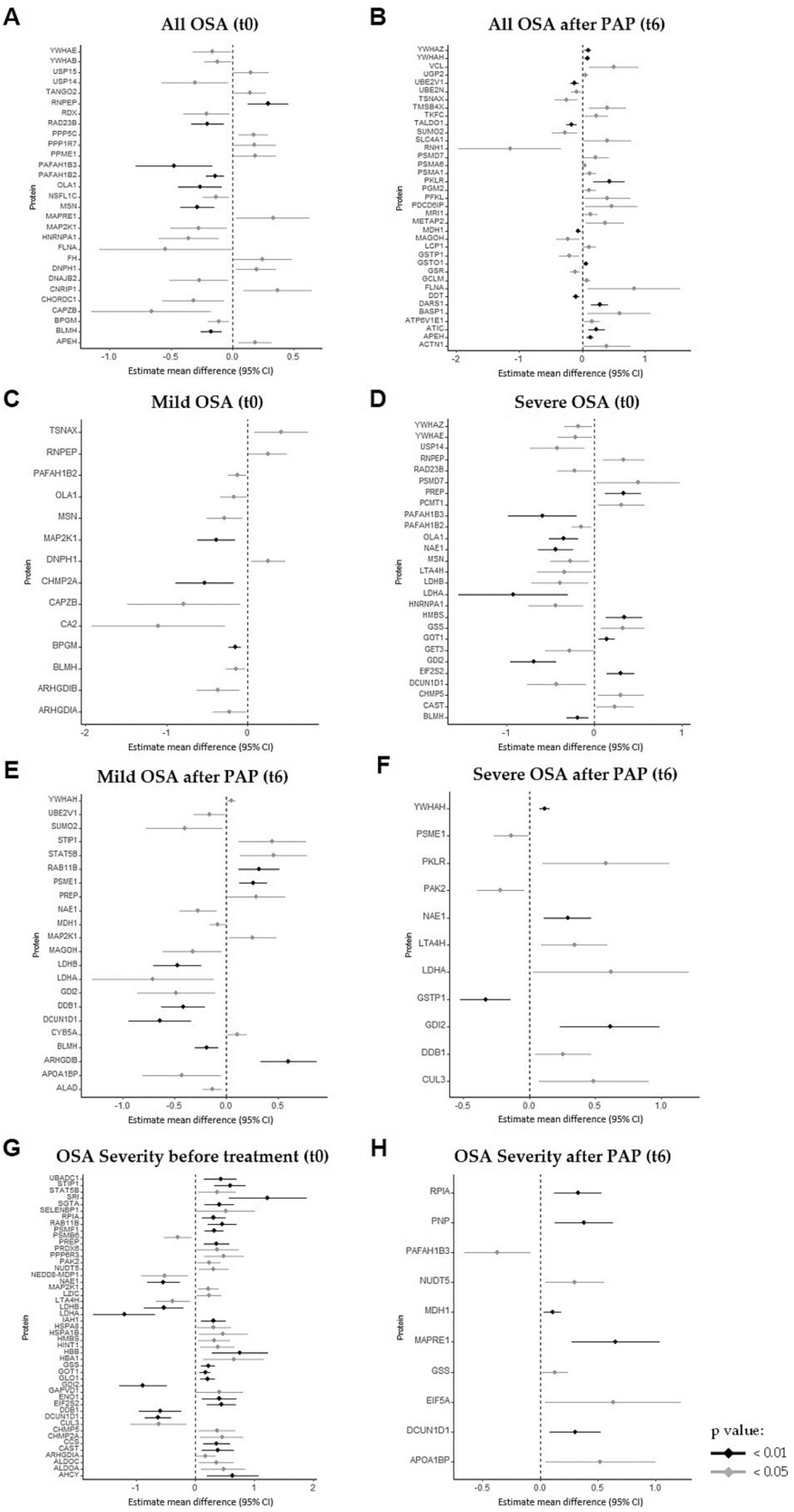

(caption on next page)

Fig. 2. Forest plots of differentially expressed proteins estimated from the linear model (LM) and linear mixed model (LMM) regression analysis. Proteins (gene name - UniProtKb) with p value < 0.01 (black) and p value < 0.05 (grey) significance threshold are shown in (A) All non-treated OSA (t0) compared with Snorers; (B) All OSA after six months of PAP treatment (t6) compared to before treatment (t0); (C) non-treated Mild OSA (t0) compared with Snorers; (D) non-treated Severe OSA (t0) compared with Snorers; (E) Mild OSA after six months of PAP treatment (t6) compared with Mild OSA before treatment (t0); (F) Severe OSA (t6) compared with Severe OSA (t0); (G) non-treated Severe OSA compared with non-treated Mild OSA; (H) PAP treated Severe OSA (t6) compared with PAP treated Mild OSA (t6). Diamonds indicate the point estimate the mean difference (mean – is the difference in effect between the study groups) and horizontal lines indicate the 95 % confidence intervals (CI) of the study results, each end of the line representing the boundaries of the confidence interval. *P* value adjustment for multiple comparisons was executed through the Dunn–Šidák correction (control family-wise error rate).

(LMM *p* value = 0.004 and p value = 0.005, respectively) and after PAP, they increased in Mild OSA (LMM p value = 0.02 and p value = 0.005, respectively), but decreased in Severe OSA (Fig. 4, A, B). Changes in ALDOA and ALDOC in response to treatment showed significant interaction with disease severity (LMM *p* value = 0.02 and p value = 0.012, respectively).

Before treatment, GAPDH was significantly lower in Severe OSA (LMM *p* value = 0.036), presenting a tendency to increase towards the levels of the control group following PAP (Fig. 4, C), while in Mild OSA, GAPDH presented no significant changes across time.

Phosphoglycerate kinase 1 (PGK1) catalyses one of the two ATP-producing reactions in the glycolytic pathway, before treatment it was shown to be lower in Severe OSA compared to Mild OSA, but this difference was not significant. However, in response to PAP treatment, it showed a significant interaction with OSA severity (LMM *p* value = 0.013) (Fig. 4, D).

The BPGM showed lower in Mild OSA compared with Severe OSA (LMM p value = 0.028) and after PAP, it increased in Mild OSA but decreased in Severe OSA respectively (was not significant) (Fig. 4, E).

Before PAP, the glycolytic alpha-enolase (ENO1) was significantly higher in Severe OSA (LMM *p* value = 0.002), while PKLR, LDHA and LDHB were lower compared to Mild OSA (LMM p value = 0.019, *p* value ≈ 0 and p value = 0.001, respectively). After treatment, ENO1 decreased in Severe OSA, but significantly increased in Mild OSA (LMM *p* value = 0.004). In contrast, PKLR, LDHA and LDHB presented an increase in Severe OSA, after treatment (LMM contrasts, p value = 0.0265 and p value = 0.042, respectively). The opposite was observed in Mild OSA, where the levels of LDHA and LDHB were lower following treatment (LMM p value = 0.007 and p value = 0.001, respectively); and no significant changes were observed for PKLR (Fig. 4, F–I).

Proteome alterations in the oxidative and non-oxidative PPP arms were also identified. The key enzyme of the oxidative PPP (oxiPPP) for the production of NADPH, the glucose-6-phosphate 1-dehydrogenase (G6PD) that was found decreased in Severe OSA compared to Mild OSA, although without statistical significance increased significantly in Severe OSA but decreased in Mild OSA in response to PAP (LMM interaction *p* value = 0.016) (Fig. 4, J).

The non-oxiPPP enzyme, RPIA, was significantly increased in Severe OSA compared to Mild OSA (LMM *p* value = 0.001), while transaldolase (TALDO1) decreased although not significantly. After PAP, RPIA increased (LMM contrasts, *p* value = 0.0035) and TALDO1 decreased in both OSA groups (LMM, Mild at t6 *p* value = 0.013 and Severe at t6 was not significant) (Fig. 4, K, L).

Associated with GSH synthesis, the proteins that showed statistical significance were lactoylglutathione lyase (GLO1), malate dehydrogenase (MDH1), GOT1, GGCT and GSS (Fig. 4, M–Q). GLO1 derives its name from its catalysis of the first step in the glyoxalase system, a critical two-step detoxification system for methylglyoxal, leading to GSH production and reutilization cycling (Fig. 4, V). Before treatment, GLO1 level was higher in Severe OSA than in Mild OSA (LMM *p* value = 0.001). After PAP, GLO1 decreased in Severe OSA but significantly increased in Mild OSA (LMM p value = 0.021), both towards Snorer level (Fig. 4, M). MDH1, GOT1, GGCT and GSS were all at higher levels in non-treated Severe OSA (LMM p value = 0.021, p value ≈ 0, p value = 0.015 and p value ≈ 0, respectively) (Fig. 4, N–Q). After PAP, MDH1 decreased significantly only in Mild OSA (LMM *p* value = 0.012) but not in Severe OSA, which increased the difference between them at t6 (LMM contrasts, p value = 0.0071). GOT1 significantly increased after PAP (LMM p value = 0.049) only in Mild OSA. Differential response to PAP showed significant for GOT1 regarding the severity (LMM p value = 0.036).

The membrane protein, band 3 anion transport protein (SLC4A1), was decreased in Mild OSA compared to Severe OSA and after treatment increased significantly (LMM p value = 0.029). Ankyrin-1 (ANK1) and erythrocyte membrane protein band 4.2 (EPB42) were also found significantly modulated between OSA severities (LMM p value = 0.013 and p value = 0.023, respectively) (Fig. 4, R–T). After PAP, ANK1 decreased only in Mild OSA, while EPB42 increased in both OSA severities but without statistical significance (Fig. 4, S, T).

Lower level of CA2 was found in Mild OSA compared with Severe OSA (LMM p value = 0.018). Following PAP, this protein decreased in both Mild OSA and Severe OSA, being most significant in the latter although without statistical significance (Fig. 4, U).

3.6. Proteins of Ubiquitin and Ubiquitin-like (Neddylation and Sumoylation) Proteasome System (UPS) were differentially modulated in OSA severity and OSA severity response to PAP treatment

Several proteins of the Ubiquitin/Ubiquitin-like (Sumoylation/Neddylation) and Proteasome System were found differentially modulated in the two spectra of OSA severity, as well as in their response to PAP treatment, estimated by LM and LMM statistical models (Figs. S2 and 5).

By comparing non-treated Mild OSA or Severe OSA with Snorers (as intercept), ten differentially expressed proteins were identified with LM *p* value < 0.05, as part of the Ubiquitination and Neddylation of the Proteasome System (Fig. S2).

The ubiquitin-conjugating enzyme E2 K (UBE2K) was higher in Mild OSA compared to Snorers control (LM p value = 0.033). Severe OSA, on the other hand, presented a decrease in the ubiquitin carboxyl-terminal hydrolase 14 (USP14), and an increase in the ubiquitin carboxyl-terminal hydrolase 15 (USP15) (LM *p* value = 0.007 and *p* value = 0.035, respectively) (Fig. S2, A–C).

The proteins of the Neddylation pathway such as the Ubiquitin-Like Protein Nedd8 (NEDD8-MDP1) and DNA damage-binding protein 1 (DDB1) were increased in Mild OSA (LM *p* value = 0.046 and p value = 0.025, respectively) (Fig. S2, D, E). In contrast, DDB1, NEDD8-activating enzyme E1 regulatory subunit (NAE1) and DCN1-like protein 1 (DCUN1D1) showed a significant decrease in Severe OSA (LM *p* value = 0.03, p value = 0.001 and p value = 0.009, respectively) (Fig. S2, E–G).

Proteins of the 20S proteasome machinery, such as the proteasome subunit beta type-6 (PSMB6) with peptidylglutamyl-hydrolyzing activity, and the proteasome subunit beta type-7 (PSMB7), displaying a trypsin-like activity were also found decreased in Severe OSA compared to Snorers (LM *p* value = 0.031 and p value = 0.041, respectively), while a protein of the 26S proteasome non-ATPase regulatory subunit 7 (PSMD7) was increased (LM *p* value = 0.023) (Fig. S2, H–J).

The LMM evaluation of the impact of PAP treatment or PAP treatment response in patients with different spectrum of OSA severity, showed also significant changes in UPS proteins across time, i.e., before and after treatment (Fig. 5).

A precursor related with the Sumoylation pathway, the small ubiquitin-related modifier 2 (SUMO2), showed a significant decrease in both Mild OSA and Severe OSA after treatment, although with statistical significance only in Mild patients (LMM *p* value = 0.01) (Fig. 5, A).

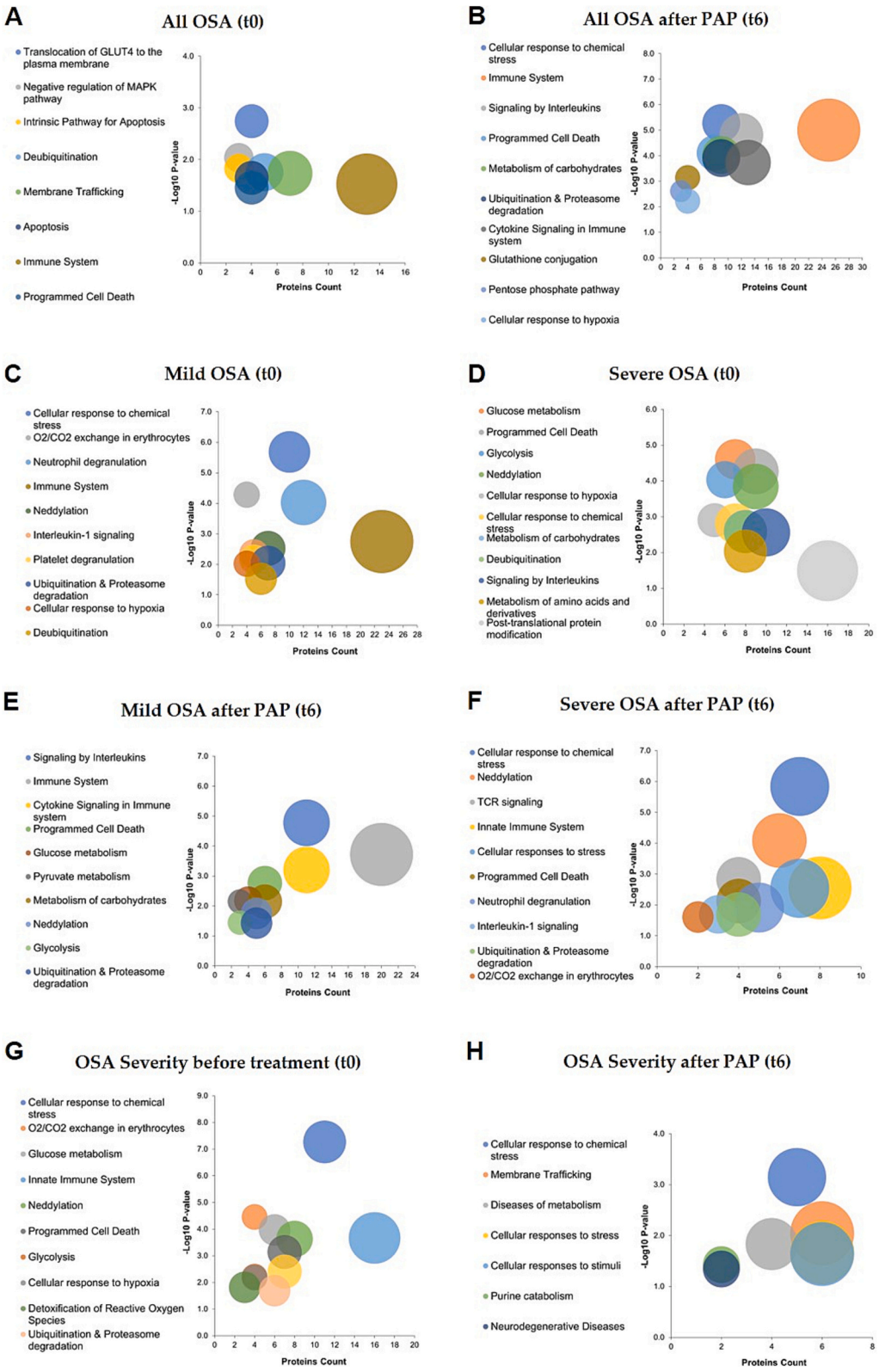

Fig. 3. Bubble plot visualization of the Reactome Pathways enrichment analysis. The most significant (p value < 0.05) Reactome pathways of the identified differentially expressed proteins are shown in (A) All non-treated OSA (t0) compared with Snorers; (B) All OSA after six months of PAP treatment (t6) compared to before treatment (t0); (C) non-treated Mild OSA (t0) compared with Snorers; (D) non-treated Severe OSA (t0) compared with Snorers; (E) Mild OSA after six months of PAP treatment (t6) compared with Mild OSA before treatment (t0); (F) Severe OSA (t6) compared with Severe OSA (t0); (G) non-treated Severe OSA (t0) compared with non-treated Mild OSA (t0); (H) PAP treated Severe OSA (t6) compared with PAP treated Mild OSA (t6). The Reactome pathways were acquired from Database for Annotation, Visualization and Integrated Discovery (DAVID) v2021.

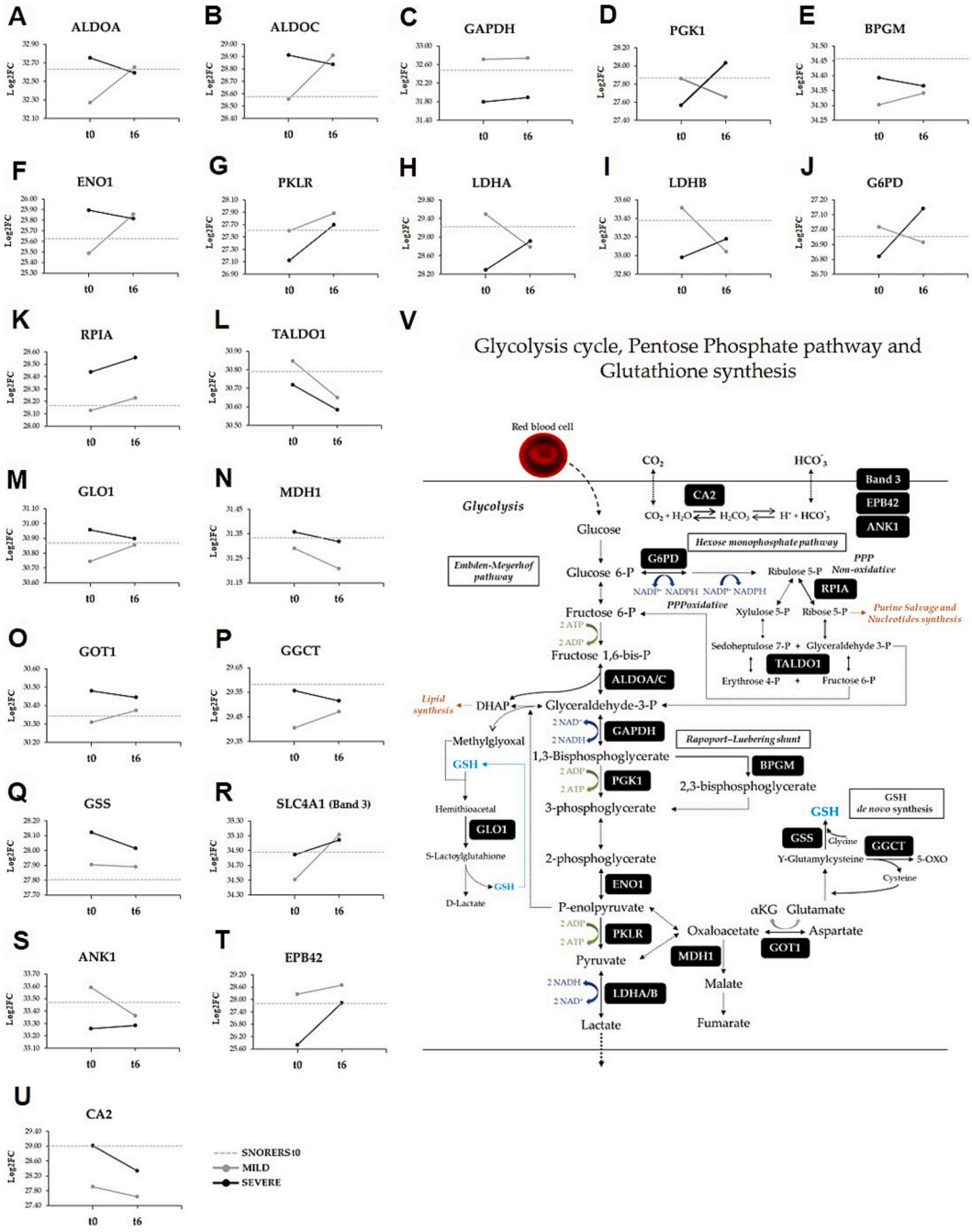

Fig. 4. Spaghetti plots of differentially expressed proteins between non-treated (t0) Mild OSA and Severe OSA and their response to PAP treatment estimated from the linear mixed model (LMM) regression analysis. Proteins of RBC glycolysis cycle, pentose phosphate pathway and glutathione synthesis, presenting statistically significant differences with a p value < 0.05 are shown. (A) Fructose-bisphosphate aldolase A, ALDOA; (B) Fructose-bisphosphate aldolase C, ALDOC; (C) Glyceraldehyde-3-phosphate dehydrogenase, GAPDH; (D) Phosphoglycerate kinase 1, PGK1; (E) Bisphosphoglycerate mutase, BPGM; (F) Alpha-enolase, ENO1; (G) Pyruvate kinase, PKLR; (H) L-lactate dehydrogenase A chain, LDHA; (I) L-lactate dehydrogenase B chain, LDHB; (J) Glucose-6-phosphate 1-dehydrogenase, G6PD; (K) Ribose-5-phosphate isomerase, RPIA; (L) Transaldolase, TALDO1; (M) Lactoylglutathione lyase, GLO1; (N) Malate dehydrogenase, cytoplasmic, MDH1; (O) Aspartate aminotransferase, GOT1; (P) Gamma-glutamylcyclotransferase, GGCT; (Q) Glutathione synthetase, GSS; (R) Band 3 anion transport protein, SLC4A1; (S) Ankyrin-1, ANK1; (T) Erythrocyte membrane protein band 4.2, EPB42; (U) Carbonic anhydrase 2, CA2. (V) Image shows the representative steps of glycolysis cycle, pentose phosphate pathway and glutathione synthesis, indicating the participation of those proteins. RBCs proteome from Mild OSA and Severe OSA, before (t0) and after six months of PAP treatment (t6) were compared using linear mixed-effects model. Mild OSA (t0) was used as intercept. The level of a protein in Snorers at steady state is indicated as reference (dashed line).

In Severe OSA, proteins of the Ubiquitination pathway such as the ubiquitin-like modifier-activating enzyme 1 (UBA1), UBE2K (p value was not significant in both) and USP14 (LMM p value $= 0.039$) were lower compared with Mild OSA but not ubiquitin-conjugating enzyme E2 variant 1 (UBE2V1). In contrast, the ubiquitin-conjugating enzyme E2 N (UBE2N) and ubiquitin-associated domain-containing protein 1 (UBADC1) were significantly higher in Severe OSA than in Mild OSA (LMM p value $= 0.035$ and p value $= 0.001$, respectively) (Fig. 5, B–G).

After PAP treatment, the UBA1, UBE2K and UBE2V1 significantly decreased only in Mild OSA (LMM p value $= 0.015$, p value $= 0.041$ and p value $= 0.012$, respectively). The UBE2N and USP14 also decreased in the RBCs of these patients, but without significance. In Severe OSA, all

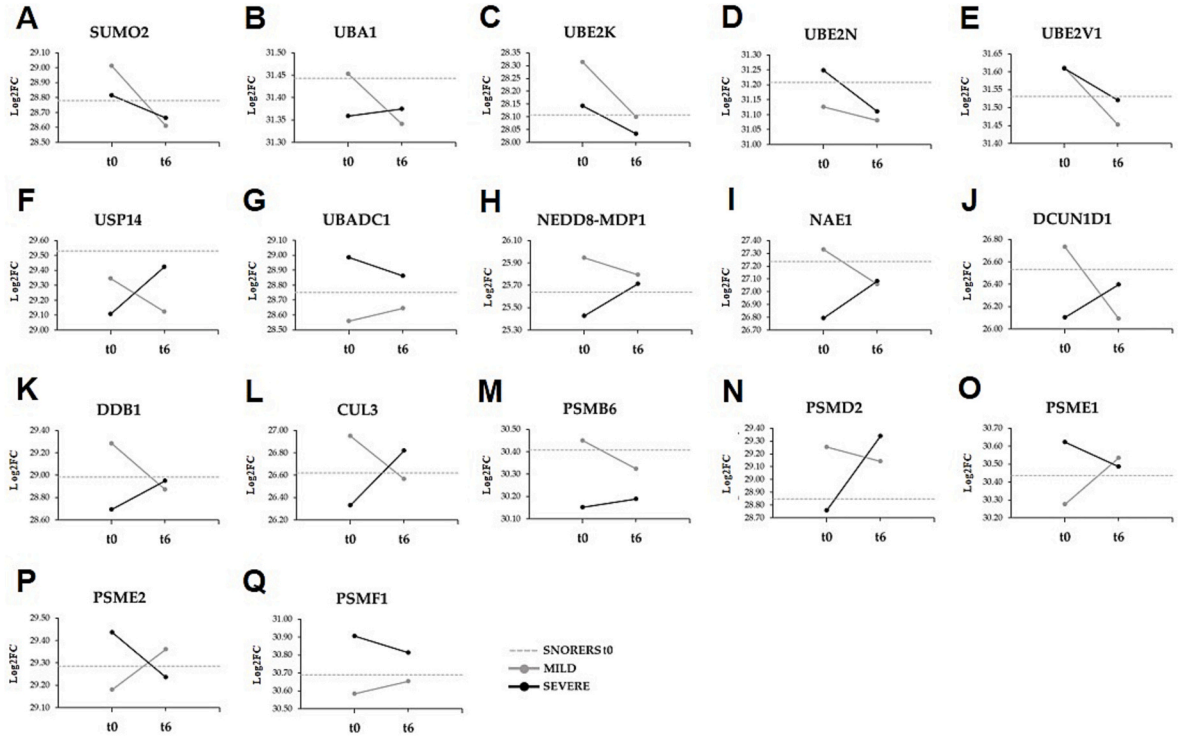

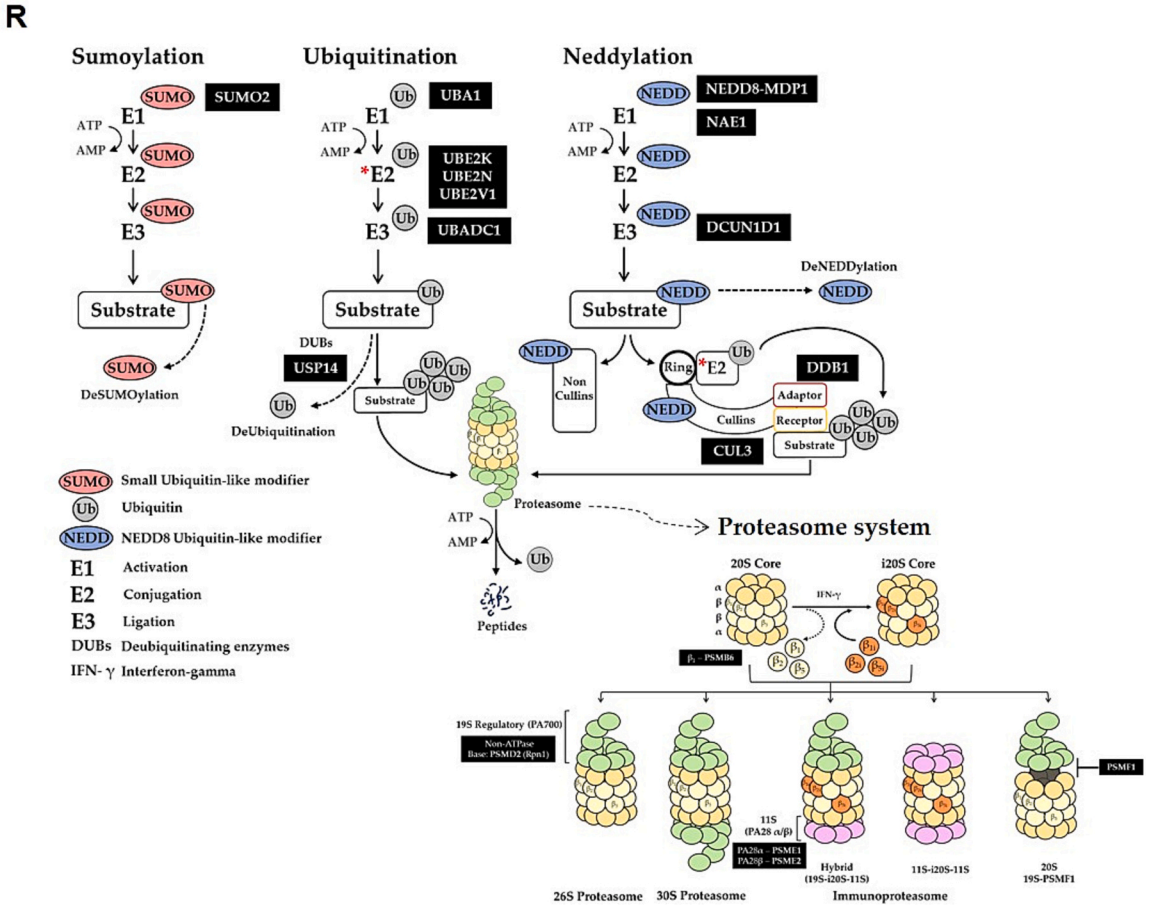

(caption on next page)

Fig. 5. Spaghetti plots of differentially expressed proteins between Mild OSA and Severe OSA, before (t0) and after six months of PAP treatment (t6) estimated from the linear mixed model (LMM) regression analysis. Proteins associated with Sumoylation, Ubiquitination, Neddylation and the ubiquitin-proteasome system, presenting statistically significant differences with a p value < 0.05 are shown. (A) Small ubiquitin-related modifier 2, SUMO2; (B) Ubiquitin-like modifier-activating enzyme 1, UBA1; (C) Ubiquitin-conjugating enzyme E2 K, UBE2K; (D) Ubiquitin-conjugating enzyme E2 N, UBE2N; (E) Ubiquitin-conjugating enzyme E2 variant 1, UBE2V1; (F) Ubiquitin carboxyl-terminal hydrolase 14, USP14; (G) Ubiquitin-associated domain-containing protein 1, UBADC1; (H) NEDD8, NEDD8-MDP1; (I) NEDD8-activating enzyme E1 regulatory subunit, NAE1; (J) DCN1-like protein 1, DCUN1D1; (K) DNA damage-binding protein 1, DDB1; (L) Cullin-3, CUL3; (M) Proteasome subunit beta type-6, PSMB6; (N) 26S proteasome non-ATPase regulatory subunit 2, PSMD2; (O) Proteasome activator complex subunit 1, PSEM1; (P) Proteasome activator complex subunit 2, PSME2; (Q) Proteasome inhibitor PI31 subunit, PSMF1; (R) Image shows the representative steps of the Sumoylation, Ubiquitination and Neddylation pathways, indicating the participation of these proteins. Conjugation of small ubiquitin-like modifier (SUMO), ubiquitin (Ub) and NEDD8 ubiquitin-like modifier (NEDD8) through an enzymatic cascade of E1, E2, and E3 ligases to protein substrates. Protein substrates ubiquitinated are degraded via the proteasome system. The structure of the proteasome and immunoproteasome is shown. The 20S proteasome is a cylindrical structure composed of two outer α - and two inner β-rings and the 19S proteasome is the regulatory cap. These two types of proteosome form the 26S/30S proteasome. In RBC there is mainly the 20S proteasome [28]. Upon stimulation with oxidative stress, the constitutively expressed catalytic β-subunits of the standard proteasome are replaced by inducible β-counterparts: β1i; β2i and β5i. They form the 20S immunoproteasome (i20S). The mature i20S then binds to either 19S proteasome (PA700), or 11S proteasome (PA28 α/β), or a combination of both proteasome activators at its two ends to form two different types of immunoproteasomes. Most prominent targets of Neddylation are cullin-RING ubiquitin ligases. Both neddylated cullin-RING and non-cullins are deneddylated by NEDD8 isopeptidases. Deubiquitination of protein substrates is mediated via deubiquitinases (DUBs). SUMOylated protein substrates are also deSUMOylated. RBCs proteome from Mild OSA and Severe OSA, before (t0) and after six months of PAP treatment (t6) were compared using a linear mixed model. Mild OSA (t0) was used as intercept. The level of a protein in Snorers at steady state is indicated as reference (dashed line).

these proteins were also decreased, except UBA1 and USP14 that showed an increase in response to PAP although without statistical significance, but the treatment response in the Severe group is inverse to the response in the Mild group (LMM p value = 0.029 and p value = 0.004, respectively) (Fig. 5, B–G).

Before PAP, the 20S proteasome PSMB6 protein with peptidylglutamyl-hydrolyzing activity and the 19S Regulatory proteasome protein, the 26S proteasome non-ATP regulatory subunit 2 (PSMD2) were decreased in Severe OSA than in Mild OSA, although with only statistical significance for the former (LMM p value = 0.004) (Fig. 5, M, N).

The activator complex subunit 1 and 2 (PSME1 and PSME2), associated with the activation by 11S proteasome (PA28 α/β) and the proteasome inhibitor PI31 subunit (PSMF1) that act by direct binding to the outer rings of the 20S proteasome or by competing with the activating particles for 20S binding [26,27], were also significantly increased in Severe OSA before PAP (LMM p value = 0.019, p value = 0.021 and p value ≈ 0, respectively) (Fig. 5, O–Q). However, after PAP an opposite modulation was observed. PSMB6 and PSMD2 exhibited an increase in Severe OSA, while in Mild OSA a decrease, but without significance (Fig. 5, M, N). PSME1, PSME2 and PSMF1 showed a decrease in Severe OSA and increase in Mild OSA, with a tendency to revert to control levels in the latter (LMM p value = 0.001, p value = 0.023 and p value = 0.042, respectively) (Fig. 5, O–Q).

4. Discussion

In the present study, the severity of OSA and the effect of six months of PAP treatment were investigated on RBC proteome by using shotgun proteomics followed by LM and LMM statistical analysis.

OSA involves repetitive episodes of hypoxia/reoxygenation and arousals events that can lead to chronic inflammation and systemic oxidative stress, an imbalance between the production of oxygen free radicals and the antioxidant capacity of the organism [29]. OSA and OSA severity have been positively correlated with several oxidative-stress biomarkers, and PAP treatment has been shown to decrease oxidative stress [30].

RBCs possess antioxidative and redox systems able to maintain intracellular homeostasis and to prevent oxidative damage and these mechanisms may be insufficient and different in patients with different spectrum of OSA severity. Antioxidant defence in RBCs plays an important role in the O_2 response in hypoxia, through glucose metabolism, which is linked to reduce equivalent recycling [31]. Anaerobic glycolysis plays pivotal roles in RBC functions since RBC depend solely on glycolysis to generate adenosine triphosphate (ATP). About 25 % of glucose in RBCs is used to produce the RBC specific metabolite 2,3-bisphosphoglycerate (2,3-BPG) for hemoglobin O_2 affinity modulation by *Rapport-Luebering* shunt of glycolysis, and RBCs depend on oxiPPP branch to generate reduced nicotinamide adenine dinucleotide phosphate (NADPH) to preserve GSH homeostasis and counteract oxidative stress [32].

The results of this study suggest that the RBCs from Severe OSA patients present a significant decrease in key glycolytic enzymes such as GAPDH, PKLR, LDHA and LDHB compared to Mild OSA. GAPDH is a recognized key redox-sensor regulating O_2-induced metabolic reroute from EMP glycolysis to oxiPPP along the normal course of RBC circulation from lung to tissues [33,34]. Reversible oxidation of GAPDH is highly relevant for the triggering of the glycolysis – oxiPPP transition and the balancing of NADPH supply in oxidative stress situations [35]. Our previous data by using 2Dgel-based proteomics, we confirmed that the redox-state of GAPDH is compromised in OSA that could be associated with OSA severity, and PAP treatment showed to revert this regulation [2].

PKLR, LDHA and LDHB regulate the rate-limiting final step of glycolysis. PKLR catalyses the transfer of a phosphate group from phosphoenolpyruvate (PEP) to adenosine diphosphate (ADP), yielding one molecule of pyruvate and two molecules of adenosine triphosphate (ATP). This process is responsible for the generation of 50 % of all ATP in RBCs [36]. Once pyruvate is produced it can be converted to L-lactate by catalyses reduction of LDHA coupled with the oxidation of NADH to NAD^+. This reaction is reverted by LDHB that converts lactate to pyruvate, and NAD^+ to NADH, when oxygen is abundant. Since glycolysis requires NAD^+, ATP production by glycolysis is hindered when NAD^+ levels diminish and NADH accumulates [37,38]. The reduction of these enzymes leads us to speculate that the generated pyruvate and lactate metabolites may be reduced, compromising the redox state and glycolytic energy metabolism in these patients. However, morning lactate levels have been shown to be modestly elevated in OSA [39], or significantly decreased in OSA patients during exercise, suggesting an impaired aerobic and glycolytic capacity in this condition similar to that seem at high altitude, where low-O_2 gas mixtures is available [40,41]. The phenomenon known as the lactate paradox, where hypoxia-acclimation-induced lowering of peak blood lactate relative to higher levels in acute hypoxia, has long been a topic of controversial debate [42].

Although we showed a decrease in those glycolytic proteins, interestingly an increase in the ENO1 in Severe OSA compared to Mild OSA was also observed.

ENO1 is a moonlight protein and plays an important role in the process of cancer development such as lung cancer, and several other diseases including Alzheimer's disease, diabetes and hypoxic-ischemic encephalopathy [43], which are comorbidities of OSA. A meta-analysis study showed that about 5 million individuals with OSA had an approximately 30 % higher risk of lung cancer compared with those

without OSA [44]. An increase in ENO1 with a decrease in PKLR may lead to accumulation of PEP substrate, known to inhibit triosephosphate isomerase (TPI) activity. TPI interconverts dihydroxyacetone phosphate (DHAP) and glyceraldehyde-3-phosphate [45]. TPI inhibition can lead to DHAP accumulation that undergoes conversion to methylglyoxal (MG), a toxic compound involved in forming advanced glycation end product. Methylglyoxal is detoxified by ubiquitous glyoxalase system, and the GLO1 enzyme involved in its detoxification, showed significantly increased in Severe OSA RBC.

TPI inhibition by the pyruvate kinase substrate phosphoenolpyruvate (PEP) in glycolysis results in the activation of PPP to counteract oxidative-stress [45]. In Severe OSA RBC, the RPIA enzyme that catalyses the reversible conversion of ribulose 5-phosphate to ribose-5-phosphate (ribose 5-P) and participates in the first step of the non-oxidative branch of PPP showed to be significantly increased, suggesting the activation of non-oxiPPP in these patients. The non-oxiPPP branch is reversible and instead to produce NADPH it can undergo purine salvage reactions, where purine bases are recycled and used in a new process [46–48]. The irreversible oxiPPP branch may not be as active as its key rate-limiting enzyme GP6D has shown a tendency to be decreased in these patients. Low oxiPPP activity impaired the capacities of RBC to handle with oxidative stress by limiting it capacity to generate NAPDH, a cofactor required for reduction of oxidized GSH or to act directly as an antioxidant [46].

Plasma level of reduced GSH, which recycling is oxiPPP dependent, was showed lower in Severe and Moderate OSA compared to Mild OSA, suggesting a reduced antioxidant capacity in these patients [49]. In Severe OSA RBC, de novo synthesis of GSH could be increased as GSS enzyme showed significantly increased compared to Snorers. It was demonstrated that the lower antioxidant capacity of hypoxic RBCs compared to normoxic ones was more related to the redox-recycling process than to de novo GSH synthesis [50]. Another study suggested that hypoxia causes an increase in GSH in RBCs [51].

Humans promote a robust series of physiological response to maintain adequate O_2 load during hypoxia [52]. At high altitude with limited O_2 concentration, the level of 2,3-BPG in RBCs increases significantly leading to a decrease of O_2 affinity by Hb, and its elevation is associated with ability of RBCs to release O_2 near tissues that need it most [41,52,53]. Contrary to our expectation, the BPGM enzyme responsible for 2,3-BPG synthesis showed significantly decreased in Mild OSA and Severe OSA. Decreased in 2,3-BPG increases O_2 affinity by Hb. Some studies have demonstrated that high Hb-O_2 affinity is a beneficial adaptation to low O_2 availability, as seen in high-altitude natives long challenged by hypoxia and also in several species exposed to high altitudes for generations [52,54]. Increased in Hb-O_2 affinity may contribute to increase ventilation and lung blood flow, enhancing O_2 uptake at the gas exchange surfaces [55]. Interestingly, the abundance of CA2 enzyme, with an important role in CO_2 influx and efflux by RBC and thus acid–base homeostasis, showed significantly downregulated only in Mild OSA RBC and not in Severe OSA RBC, compared with controls. CA activity has been positively associated with OSA severity, showing significantly activated in Severe OSA compared with controls or Mild OSA [56], and PAP did not change CA activity [57]. No difference in the CA activity per millilitre of RBCs has been found between the sea level and high-altitude natives [58]. CA inhibitors have been used in the treatment of many diseases, including acute mountain sickness and sleep apnea syndrome [58,59].

Therapy with PAP reduces hypoxia/reoxygenation events and therefore oxidative stress in OSA [2,60], which might have a significant beneficial impact on OSA RBC metabolism [2]. Our results indicate that six months of PAP treatment may restore the glycolysis metabolism in RBC that was particularly modulated in Severe OSA patients before treatment. After PAP, the glycolytic enzymes PKLR, LDHA and LDHB increased significantly in Severe OSA RBC to levels closer to those of Snorers. Furthermore, the effect of the treatment also increased the production of the PGK1, an important enzyme that generates ATP in glycolysis, unlike Mild OSA at t6. The oxiPPP key rate-limiting enzyme GP6D as well as the non-oxiPPP RPIA enzyme, showed significantly increased after PAP. Taken together these data suggested PAP induced ATP energy metabolism, antioxidant defence and purine salvage pathways in RBC of patients with Severe OSA.

In Mild OSA, although the glycolytic enzymes such as ALDOA, ALDOC, ENO1, and PKLR increased significantly after PAP, LDHA and LDHB enzymes of the final step of glycolysis showed significantly decreased. The pyruvate produced may not be sufficiently catalysed to lactate in Mild patients under the effect of PAP. In contrast to what was observed in Severe OSA, GP6D showed a slight decreased in Mild OSA RBC after PAP. Future investigations will be need to better understand these changes involved in RBCs homeostasis in Mild and Severe OSA conditions, and their response to PAP therapy.

In this study, proteins related to UPS system, which plays an important role in the regulation of protein stability and function, were also showed modulated in OSA severity and response to PAP treatment. The process of ubiquitination keeps protein functional states in a homeostatic balance [61]. Proteins are modified not only by the addition of small chemical moieties but also by covalent attachment of short modifier proteins such as ubiquitin, small ubiquitin-like modifier (SUMO) or other ubiquitin-like proteins (UBLs), such as NEDD8. It was reported that the sequences of NEDD8 and ubiquitin are 59 % identical [62]. The ubiquitin-like molecule NEDD8 is a regulator of multitude of biological processes both under homeostatic and proteotoxic stress conditions [63,64]. Our results suggest that ubiquitination and ubiquitin-like pathways were less pronounced in Severe OSA than in Mild OSA compared to Snorers. NAE1, DCUN1D1, DDB1 and USP14 proteins were significantly decreased in Severe OSA compared to Mild OSA or Snorer group.

It is known that ubiquitination and ubiquitin-like pathways are an ATP-dependent cascade process that binds ubiquitin [62,65,66]. Molecular O_2 is essential for the production of ATP in human cells and its deficiency leads to a reduction in the energy levels that are required to preserve biological functions [67]. In OSA RBCs, to generate ATP, glucose metabolism must be active, and our results indicated that glycolysis was compromised in Severe OSA but not in Mild OSA. In patients with Mild OSA, there was overexpression of proteins related to ubiquitination and neddylation, such as UBE2K, NEDD8-MDP1 and DDB1.

In Severe OSA, the proteins PSMB6 (β1) and PSMB7 (β2), associated with the core 20S proteasome showed a significant decrease. Interestingly, PSME1 and PSME2 proteins associated with core 20S regulators such as the PA28α and PA28β complex, respectively, were increased in Severe OSA compared to Mild OSA. It is known that during episodes of acute stress, the 19S regulatory lid of the 26S proteasome separates from the proteolytic core, and is immediately followed by ATP/ubiquitin-independent protein degradation by the 20S proteasome [68]. There are studies that show that the regulator PA28 (11S) can significantly improve the ability of the 20S proteasome to selectively degrade oxidized protein substrates, and that the immunoproteasome can be even more effective [68]. Our findings suggest that this may be occurring in RBCs of patients with Severe OSA, as immunoproteasomes display higher specific activity, as well as a greater capacity to degrade oxidized proteins [69]. Another study showed that mild oxidative stress increases levels of ubiquitin conjugates in many types of cells and tissues, whereas extensive oxidative stress reduces the levels of ubiquitin conjugates [70]. Recent evidences have shown that the immunoproteasome is an important player in the removal of damaged proteins in cellular homeostasis, and especially during stress conditions and disease [69,71].

Taken together, these data raise the hypothesis that immunoproteasome may be activated in Severe OSA RBC to counteract severe intermittent nocturnal hypoxia – induced oxidative stress. The 20S proteasome is relatively resistant to oxidative stress and maintains its activity under conditions in which protein damage occurs, whereas the

26S proteasome and the ubiquitination pathway are much more susceptible to conditions of oxidative stress [69,72,73].

PAP treatment induced modulation in those UPS proteins showing interaction with OSA severity. PAP treatment reduced the immunoproteasome system in Severe OSA. A significant decrease in PSME1 and PSME2, and a significant increase in NAE1, DCUN1D1, cullin-3 (CUL3) and PSMD2 proteins after PAP treatment were observed in Severe OSA. These data suggest that to maintain RBC homeostasis, degradation of oxidized proteins is upregulated after PAP through the neddylation and ubiquitination system, because neddylation is a regulator of biological processes essential for cell viability, development and responses to stress, and therefore is a promising route for therapeutic intervention [64,74]. In Mild OSA, PAP treatment induced a decrease in proteins related to ubiquitination and neddylation, but appears to cause an increase in the immunoproteasome system, PSME1 and PSME2 proteins, suggesting that the effect of PAP treatment in this severity group may induce oxidative stress in Mild OSA RBC. This result meets the question about the use of PAP as a first-line treatment for patients with Mild OSA [75,76].

Limitations in this study should be addressed. Sample size, female gender exclusion, the OSA group being constituted by non-diabetics but with higher levels of blood insulin and HOMA-IR, BMI and abdominal circumference limit the data generalization. Although patients were instructed to follow a restricted diet for three days before urine/blood collection to minimize its impact in patient's antioxidant status and catecholamine determination, their dietary habits were not fully controlled. Proteomics and validation analysis were performed on −80 °C stored samples, which could introduce some bias in the molecular events of both control and disease samples.

5. Conclusion

The EMP and PPP interconversion pathways of glycolysis showed to be higher deregulated in RBCs from patients with Severe clinical manifestation of OSA than in patients with Mild disease.

RBC glycolysis as source of energy and antioxidant reducing agents may be compromised in patients with Severe OSA in response to severe intermittent nocturnal hypoxia/reoxygenation – induced oxidative stress.

The antioxidant capacity of RBCs may also be under challenge in Severe OSA, as indicated by deregulation in oxiPPP enzymes that generate reducing agents associated with upregulation of non-oxiPPP enzymes towards purine salvage pathway. Enzymes associated with de novo GSH synthesis also showed upregulated in Severe OSA RBC.

Downregulation of the *Rapoport-Luebering* glycolytic shunt leading to increased Hb-O_2 affinity may be a beneficial adaptation in OSA, although dysregulation in EMP glycolysis was significant only in patients with Severe OSA.

In RBCs, the proteolysis by the 20S proteasome may constitute a dominant pathway for protein turnover, however, under conditions of oxidative stress, alternative proteasome complex forms may take place.

In Severe OSA patients, the Immunoproteasome may be activated in RBC as important cellular homeostasis player to counteract severe – induced oxidative stress. In contrast, in Mild OSA patients, the upregulation of the ubiquitination/neddylation-dependent proteasome may be taking place in response to oxidative stress. Proteasome regulation in RBCs in response to different degree of OSA severity – induced oxidative stress deserved further investigation.

PAP treatment showed a beneficial impact on Severe OSA RBC metabolism by promoting energy and reducing-agents production, the reactivation of the 20S proteasome system and the upregulation of Hb-O_2 affinity in these cells.

In patients with Mild OSA, immunoproteasome proteins increased after PAP treatment. PAP may also induce downregulation in glycolysis lactate production in Mild OSA RBC. These data suggests that PAP treatment may cause an overload of oxidative stress in patients with Mild OSA disease and, therefore, the use of PAP may have to be revised or readjusted according to the degree of severity of OSA.

Further validation associated with metabolomic studies in a large cohort of patients will be needed to better understand the functional impact of these findings. The identified differentially modulated proteins may be new candidate biomarkers for diagnosis and prognosis of OSA severity or to support monitoring and efficacy of PAP treatment in OSA patients with different degrees of disease severity.

Supplementary data to this article can be found online at https://doi.org/10.1016/j.bbadis.2025.167767.

CRediT authorship contribution statement

Cristina Valentim-Coelho: Writing – review & editing, Writing – original draft, Methodology, Investigation, Formal analysis, Data curation. **Joana Saraiva:** Methodology, Investigation, Formal analysis. **Hugo Osório:** Methodology. **Marília Antunes:** Methodology, Formal analysis. **Fátima Vaz:** Methodology, Investigation, Data curation. **Sofia Neves:** Methodology, Formal analysis. **Paula Pinto:** Resources, Project administration. **Cristina Bárbara:** Resources, Project administration. **Deborah Penque:** Writing – review & editing, Writing – original draft, Supervision, Project administration, Methodology, Investigation, Funding acquisition, Conceptualization.

Ethics

The protocol of this project was approved by the Ethics Committees of the Centro Hospitalar Lisboa Norte (CHLN), Hospital Santa Maria, Lisboa, Portugal and Instituto Nacional de Saúde Dr. Ricardo Jorge, Lisboa, Portugal. The project was registered at the Comissão Nacional de Proteção de Dados (CNPD) and all patients gave written informed consent.

Funding

Project partially supported by Harvard Medical School – Portugal Program (HMSPICJ/0022/2011), Instituto Nacional de Saúde Dr. Ricardo Jorge – INSA, Centro de Toxicogenómica e Saúde Humana – ToxOmics, Rede Nacional de Espectrometria de Massa – RNEM, FCT/Poly-Annual Funding Program and FEDER/Saúde XXI Program, Portugal. Cristina Coelho (SFRH/BD/133511/2017) and Joana Saraiva (2022.14435.BD) were granted with PhD fellowships from Fundação para a Ciência e a Tecnologia – FCT. Research by Marília Antunes is partially financed by national funds through FCT under the project UIDB/00006/2020 - (doi:10.54499/UIDB/00006/2020).

Declaration of competing interest

The authors declare that they have no known competing financial interests or personal relationships that could have appeared to influence the work reported in this paper.

Acknowledgements

To patients that voluntarily collaborated in this study.

Data availability

Data will be made available on request.

References

[1] A.V. Benjafield, N.T. Ayas, P.R. Eastwood, R. Heinzer, M.S.M. Ip, M.J. Morrell, C. M. Nunez, S.R. Patel, T. Penzel, J.-L. Pépin, P.E. Peppard, S. Sinha, S. Tufik, K. Valentine, A. Malhotra, Estimation of the global prevalence and burden of obstructive sleep apnoea: a literature-based analysis, lancet, Respir. Med. 7 (2019) 687–698, https://doi.org/10.1016/S2213-2600(19)30198-5.

[2] C. Valentim-Coelho, F. Vaz, M. Antunes, S. Neves, I.L. Martins, H. Osório, A. Feliciano, P. Pinto, C. Bárbara, D. Penque, Redox–oligomeric state of peroxiredoxin-2 and glyceraldehyde-3-phosphate dehydrogenase in obstructive sleep apnea red blood cells under positive airway pressure therapy, Antioxidants 9 (2020) 1184, https://doi.org/10.3390/antiox9121184.

[3] S.R. Patel, Obstructive sleep apnea, Ann. Intern. Med. 171 (2019), https://doi.org/10.7326/AITC201912030.

[4] M. Marin-Oto, E.E. Vicente, J.M. Marin, Long term management of obstructive sleep apnea and its comorbidities, Multidiscip. Respir. Med. 14 (2019) 21, https://doi.org/10.1186/s40248-019-0186-3.

[5] J.J. Lee, K.M. Sundar, Evaluation and management of adults with obstructive sleep apnea syndrome, Lung 199 (2021) 87–101, https://doi.org/10.1007/s00408-021-00426-w.

[6] J. Pinto, D. Ribeiro, A. Cavallini, C. Duarte, G. Freitas, Comorbidities associated with obstructive sleep apnea: a retrospective study, Int Arch Otorhinolaryngol 20 (2016) 145–150, https://doi.org/10.1055/s-0036-1579546.

[7] J.S. Virk, B. Kotecha, When continuous positive airway pressure (CPAP) fails, J. Thorac. Dis. 8 (2016) E1112–E1121, https://doi.org/10.21037/jtd.2016.09.67.

[8] W.E. Fleming, J.-E.C. Holty, R.K. Bogan, D. Hwang, A.S. Ferouz-Colborn, R. Budhiraja, S. Redline, E. Mensah-Osman, N.I. Osman, Q. Li, A. Azad, S. Podolak, M.K. Samoszuk, A.B. Cruz, Y. Bai, J. Lu, J.S. Riley, P.C. Southwick, Use of blood biomarkers to screen for obstructive sleep apnea, Nat Sci Sleep 10 (2018) 159–167, https://doi.org/10.2147/NSS.S164488.

[9] T. Nemkov, J.A. Reisz, Y. Xia, J.C. Zimring, A. D'Alessandro, Red blood cells as an organ? How deep omics characterization of the most abundant cell in the human body highlights other systemic metabolic functions beyond oxygen transport, Expert Rev Proteomics 15 (2018) 855–864, https://doi.org/10.1080/14789450.2018.1531710.

[10] M.M. Cortese-Krott, The reactive species interactome in red blood cells: oxidants, antioxidants, and molecular targets, Antioxidants 12 (2023) 1736, https://doi.org/10.3390/antiox12091736.

[11] A. Mahdi, M.M. Cortese-Krott, M. Kelm, N. Li, J. Pernow, Novel perspectives on redox signaling in red blood cells and platelets in cardiovascular disease, Free Radic. Biol. Med. 168 (2021) 95–109, https://doi.org/10.1016/j.freeradbiomed.2021.03.020.

[12] V. Kuhn, L. Diederich, T.C.S. Keller, C.M. Kramer, W. Lückstädt, C. Panknin, T. Suvorava, B.E. Isakson, M. Kelm, M.M. Cortese-Krott, Red blood cell function and dysfunction: redox regulation, nitric oxide metabolism, anemia, Antioxid. Redox Signal. 26 (2017) 718–742, https://doi.org/10.1089/ars.2016.6954.

[13] A. Feliciano, F. Vaz, V.M. Torres, C. Valentim-Coelho, R. Silva, V. Prosinecki, B. M. Alexandre, A.S. Carvalho, R. Matthiesen, A. Malhotra, P. Pinto, C. Bárbara, D. Penque, Evening and morning peroxiredoxin-2 redox/oligomeric state changes in obstructive sleep apnea red blood cells: correlation with polysomnographic and metabolic parameters, Biochim. Biophys. Acta (BBA) - Mol. Basis Dis. 1863 (2017) 621–629, https://doi.org/10.1016/j.bbadis.2016.11.019.

[14] A. Feliciano, F. Vaz, C. Valentim-Coelho, V.M. Torres, R. Silva, V. Prosinecki, B. M. Alexandre, A. Almeida, C. Almeida-Marques, A.S. Carvalho, R. Matthiesen, A. Malhotra, P. Pinto, C. Bárbara, D. Penque, Evening and morning alterations in Obstructive Sleep Apnea red blood cell proteome, Data Brief 11 (2017) 103–110, https://doi.org/10.1016/j.dib.2017.01.005.

[15] A. Feliciano, V.M. Torres, F. Vaz, A.S. Carvalho, R. Matthiesen, P. Pinto, A. Malhotra, C. Bárbara, D. Penque, Overview of proteomics studies in obstructive sleep apnea, Sleep Med. 16 (2015) 437–445, https://doi.org/10.1016/j.sleep.2014.11.014.

[16] J. Cox, M. Mann, MaxQuant enables high peptide identification rates, individualized p.p.b.-range mass accuracies and proteome-wide protein quantification, Nat. Biotechnol. 26 (2008) 1367–1372, https://doi.org/10.1038/nbt.1511.

[17] S. Tyanova, T. Temu, P. Sinitcyn, A. Carlson, M.Y. Hein, T. Geiger, M. Mann, J. Cox, The Perseus computational platform for comprehensive analysis of (prote) omics data, Nat. Methods 13 (2016) 731–740, https://doi.org/10.1038/nmeth.3901.

[18] B.T. Sherman, M. Hao, J. Qiu, X. Jiao, M.W. Baseler, H.C. Lane, T. Imamichi, W. Chang, DAVID: a web server for functional enrichment analysis and functional annotation of gene lists (2021 update), Nucleic Acids Res. 50 (2022) W216–W221, https://doi.org/10.1093/nar/gkac194.

[19] A. Kuznetsova, P.B. Brockhoff, R.H.B. Christensen, lmerTest package: tests in linear mixed effects models, J. Stat. Softw. 82 (2017), https://doi.org/10.18637/jss.v082.i13.

[20] D. Bates, M. Mächler, B. Bolker, S. Walker, Fitting linear mixed-effects models using lme4, J. Stat. Softw. 67 (2015), https://doi.org/10.18637/jss.v067.i01.

[21] S.R. Searle, F.M. Speed, G.A. Milliken, Population marginal means in the linear model: an alternative to least squares means, Am. Stat. 34 (1980) 216–221, https://doi.org/10.1080/00031305.1980.10483031.

[22] Z. Sidak, Rectangular confidence regions for the means of multivariate normal distributions, J. Am. Stat. Assoc. 62 (1967) 626, https://doi.org/10.2307/2283989.

[23] H. Wickham, ggplot2, 2nd ed., Springer International Publishing, Cham, 2016 https://doi.org/10.1007/978-3-319-24277-4.

[24] H. Wickham, M. Averick, J. Bryan, W. Chang, L. McGowan, R. François, G. Grolemund, A. Hayes, L. Henry, J. Hester, M. Kuhn, T. Pedersen, E. Miller, S. Bache, K. Müller, J. Ooms, D. Robinson, D. Seidel, V. Spinu, K. Takahashi, D. Vaughan, C. Wilke, K. Woo, H. Yutani, Welcome to the Tidyverse, J Open Source Softw 4 (2019) 1686, https://doi.org/10.21105/joss.01686.

[25] H. Wickham, R. François, L. Henry, K. Müller, D. Vaughan, dplyr: a grammar of data manipulation. https://dplyr.tidyverse.org, 2023. (Accessed 25 January 2024).

[26] N. Albornoz, H. Bustamante, A. Soza, P. Burgos, Cellular responses to proteasome inhibition: molecular mechanisms and beyond, Int. J. Mol. Sci. 20 (2019) 3379, https://doi.org/10.3390/ijms20143379.

[27] H.-C. Hsu, J. Wang, A. Kjellgren, H. Li, G.N. DeMartino, High-resolution structure of mammalian PI31–20S proteasome complex reveals mechanism of proteasome inhibition, J. Biol. Chem. 299 (2023) 104862, https://doi.org/10.1016/j.jbc.2023.104862.

[28] W. Sae-Lee, C.L. McCafferty, E.J. Verbeke, P.C. Havugimana, O. Papoulas, C. D. McWhite, J.R. Houser, K. Vanuytsel, G.J. Murphy, K. Drew, A. Emili, D. W. Taylor, E.M. Marcotte, The protein organization of a red blood cell, Cell Rep. 40 (2022) 111103, https://doi.org/10.1016/j.celrep.2022.111103.

[29] A. Maniaci, G. Iannella, S. Cocuzza, C. Vicini, G. Magliulo, S. Ferlito, G. Cammaroto, G. Meccariello, A. De Vito, A. Nicolai, A. Pace, M. Artico, S. Taurone, Oxidative stress and inflammation biomarker expression in obstructive sleep apnea patients, J. Clin. Med. 10 (2021) 277, https://doi.org/10.3390/jcm10020277.

[30] A. Stanek, K. Brożyna-Tkaczyk, W. Myśliński, Oxidative stress markers among obstructive sleep apnea patients, Oxid. Med. Cell. Longev. 2021 (2021) 1–8, https://doi.org/10.1155/2021/9681595.

[31] S.C. Rogers, A. Said, D. Corcuera, D. McLaughlin, P. Kell, A. Doctor, Hypoxia limits antioxidant capacity in red blood cells by altering glycolytic pathway dominance, FASEB J. 23 (2009) 3159–3170, https://doi.org/10.1096/fj.09-130666.

[32] K. Sun, A. D'alessandro, Y. Xia, Purinergic control of red blood cell metabolism: novel strategies to improve red cell storage quality, Blood Transfus. 15 (2017) 535–542, https://doi.org/10.2450/2017.0366-16.

[33] A. Kuehne, H. Emmert, J. Soehle, M. Winnefeld, F. Fischer, H. Wenck, S. Gallinat, L. Terstegen, R. Lucius, J. Hildebrand, N. Zamboni, Acute activation of oxidative pentose phosphate pathway as first-line response to oxidative stress in human skin cells, Mol. Cell 59 (2015) 359–371, https://doi.org/10.1016/j.molcel.2015.06.017.

[34] T.P. Dick, M. Ralser, Metabolic remodeling in times of stress: who shoots faster than his shadow? Mol. Cell 59 (2015) 519–521, https://doi.org/10.1016/j.molcel.2015.08.002.

[35] D. Talwar, C.G. Miller, J. Grossmann, L. Szyrwiel, T. Schwecke, V. Demichev, A.-M. Mikecin Drazic, A. Mayakonda, P. Lutsik, C. Veith, M.D. Milsom, K. Müller-Decker, M. Mülleder, M. Ralser, T.P. Dick, The GAPDH redox switch safeguards reductive capacity and enables survival of stressed tumour cells, Nat. Metab. 5 (2023) 660–676, https://doi.org/10.1038/s42255-023-00781-3.

[36] W.J. Israelsen, M.G. Vander Heiden, Pyruvate kinase: function, regulation and role in cancer, Semin. Cell Dev. Biol. 43 (2015) 43–51, https://doi.org/10.1016/j.semcdb.2015.08.004.

[37] L.R. Gray, S.C. Tompkins, E.B. Taylor, Regulation of pyruvate metabolism and human disease, Cell. Mol. Life Sci. 71 (2014) 2577–2604, https://doi.org/10.1007/s00018-013-1539-2.

[38] R. van Wijk, W.W. van Solinge, The energy-less red blood cell is lost: erythrocyte enzyme abnormalities of glycolysis, Blood 106 (2005) 4034–4042, https://doi.org/10.1182/blood-2005-04-1622.

[39] O.A. Mesarwi, E.V. Sharma, J.C. Jun, V.Y. Polotsky, Metabolic dysfunction in obstructive sleep apnea: a critical examination of underlying mechanisms, Sleep Biol. Rhythms 13 (2015) 2–17, https://doi.org/10.1111/sbr.12078.

[40] T.A. Powell, V. Mysliwiec, M.S. Brock, M.J. Morris, OSA and cardiorespiratory fitness: a review, J. Clin. Sleep Med. 18 (2022) 279–288, https://doi.org/10.5664/jcsm.9628.

[41] A. D'Alessandro, T. Nemkov, K. Sun, H. Liu, A. Song, A.A. Monte, A.W. Subudhi, A. T. Lovering, D. Dvorkin, C.G. Julian, C.G. Kevil, G.K. Kolluru, S. Shiva, M. T. Gladwin, Y. Xia, K.C. Hansen, R.C. Roach, AltitudeOmics: red blood cell metabolic adaptation to high altitude hypoxia, J. Proteome Res. 15 (2016) 3883–3895, https://doi.org/10.1021/acs.jproteome.6b00733.

[42] M.F. Bartlett, R.A. Lehnhard, The lactate paradox: a review, Comp Exerc Physiol 7 (2010) 1–13, https://doi.org/10.1017/S1755254010000176.

[43] G. Qiao, A. Wu, X. Chen, Y. Tian, X. Lin, Enolase 1, a moonlighting protein, as a potential target for cancer treatment, Int. J. Biol. Sci. 17 (2021) 3981–3992, https://doi.org/10.7150/ijbs.63556.

[44] A.J.Y. Cheong, B.K.J. Tan, Y.H. Teo, N.K.W. Tan, D.W.T. Yap, C.-H. Sia, T.H. Ong, L.C. Leow, A. See, S.T. Toh, Obstructive sleep apnea and lung cancer: a systematic review and meta-analysis, Ann. Am. Thorac. Soc. 19 (2022) 469–475, https://doi.org/10.1513/AnnalsATS.202108-960OC.

[45] N.-M. Grüning, D. Du, M.A. Keller, B.F. Luisi, M. Ralser, Inhibition of triosephosphate isomerase by phosphoenolpyruvate in the feedback-regulation of glycolysis, Open Biol. 4 (2014) 130232, https://doi.org/10.1098/rsob.130232.

[46] M. Kirsch, H. Groot, NAD(P)H, a directly operating antioxidant? FASEB J. 15 (2001) 1569–1574, https://doi.org/10.1096/fj.00-0823hyp.

[47] A. Stincone, A. Prigione, T. Cramer, M.M.C. Wamelink, K. Campbell, E. Cheung, V. Olin-Sandoval, N. Grüning, A. Krüger, M. Tauqeer Alam, M.A. Keller, M. Breitenbach, K.M. Brindle, J.D. Rabinowitz, M. Ralser, The return of metabolism: biochemistry and physiology of the pentose phosphate pathway, Biol. Rev. 90 (2015) 927–963, https://doi.org/10.1111/brv.12140.

[48] P.N. Chatzinikolaou, N.V. Margaritelis, V. Paschalis, A.A. Theodorou, I.S. Vrabas, A. Kyparos, A. D'Alessandro, M.G. Nikolaidis, Erythrocyte metabolism, Acta Physiol. 240 (2024), https://doi.org/10.1111/apha.14081.

[49] I. Cekerevac, V. Jakovljevic, V. Zivkovic, M. Petrovic, V. Cupurdija, L. Novkovic, Impact of severity of obstructive sleep apnea (OSA) and body composition on redox status in OSA patients, Vojnosanit. Pregl. 75 (2018) 1089–1093, https://doi.org/10.2298/VSP161030041C.

[50] Y. Wang, N. Zhao, Y. Xiong, J. Zhang, D. Zhao, Y. Yin, L. Song, Y. Yin, J. Wang, X. Luan, Y. Xiong, Downregulated recycling process but not de novo synthesis of

glutathione limits antioxidant capacity of erythrocytes in hypoxia, Oxid. Med. Cell. Longev. 2020 (2020) 1–17, https://doi.org/10.1155/2020/7834252.
[51] S. Fenk, E.V. Melnikova, A.A. Anashkina, Y.M. Poluektov, P.I. Zaripov, V. A. Mitkevich, Y.V. Tkachev, L. Kaestner, G. Minetti, H. Mairbäurl, J.S. Goede, A. A. Makarov, I.Y. Petrushanko, A. Bogdanova, Hemoglobin is an oxygen-dependent glutathione buffer adapting the intracellular reduced glutathione levels to oxygen availability, Redox Biol. 58 (2022) 102535, https://doi.org/10.1016/j.redox.2022.102535.
[52] K.L. Webb, P.B. Dominelli, S.E. Baker, S.A. Klassen, M.J. Joyner, J.W. Senefeld, C. C. Wiggins, Influence of high hemoglobin-oxygen affinity on humans during hypoxia, Front. Physiol. 12 (2022), https://doi.org/10.3389/fphys.2021.763933.
[53] H. Liu, Y. Zhang, H. Wu, A. D'Alessandro, G.G. Yegutkin, A. Song, K. Sun, J. Li, N.-Y. Cheng, A. Huang, Y. Edward Wen, T.T. Weng, F. Luo, T. Nemkov, H. Sun, R. E. Kellems, H. Karmouty-Quintana, K.C. Hansen, B. Zhao, A.W. Subudhi, S. Jameson-Van Houten, C.G. Julian, A.T. Lovering, H.K. Eltzschig, M. R. Blackburn, R.C. Roach, Y. Xia, Beneficial role of erythrocyte adenosine A2B receptor–mediated AMP-activated protein kinase activation in high-altitude hypoxia, Circulation 134 (2016) 405–421, https://doi.org/10.1161/CIRCULATIONAHA.116.021311.
[54] A. Jendroszek, H. Malte, C.B. Overgaard, K. Beedholm, C. Natarajan, R.E. Weber, J. F. Storz, A. Fago, Allosteric mechanisms underlying the adaptive increase in hemoglobin-oxygen affinity of the bar-headed goose, J. Exp. Biol. (2018), https://doi.org/10.1242/jeb.185470.
[55] H. Mairbäurl, R.E. Weber, Oxygen transport by hemoglobin, in: Compr Physiol, Wiley, 2012, pp. 1463–1489, https://doi.org/10.1002/cphy.c080113.
[56] T. Wang, D. Eskandari, D. Zou, L. Grote, J. Hedner, Increased carbonic anhydrase activity is associated with sleep apnea severity and related hypoxemia, Sleep 38 (2015) 1067–1073, https://doi.org/10.5665/sleep.4814.
[57] E. Hoff, D. Zou, S. Schiza, Y. Demir, L. Grote, I. Bouloukaki, Ş. Beydemir, D. Eskandari, K. Stenlöf, J. Hedner, Carbonic anhydrase, obstructive sleep apnea and hypertension: effects of intervention, J. Sleep Res. 29 (2020), https://doi.org/10.1111/jsr.12956.
[58] J. Gamboa, R. Caceda, A. Gamboa, C. Monge-c, Carbonic anhydrase activity in the red blood cells of sea level and high altitude natives, Biol. Res. 33 (2000), https://doi.org/10.4067/S0716-97602000000300006.
[59] C.B. Mishra, M. Tiwari, C.T. Supuran, Progress in the development of human carbonic anhydrase inhibitors and their pharmacological applications: where are we today? Med. Res. Rev. 40 (2020) 2485–2565, https://doi.org/10.1002/med.21713.
[60] Renjun Lv, Xueying Liu, Yue Zhang, Na Dong, Xiao Wang, He Yao, Hongmei Yue, Qingqing Yin, Pathophysiological mechanisms and therapeutic approaches in obstructive sleep apnea syndrome, Sig. Transduct. Target. Ther. 8 (2023) 218, https://doi.org/10.1038/s41392-023-01496-3.
[61] M. Wirth, M. Schick, U. Keller, J. Krönke, Ubiquitination and ubiquitin-like modifications in multiple myeloma: biology and therapy, Cancers (Basel) 12 (2020) 3764, https://doi.org/10.3390/cancers12123764.
[62] J. Zhu, F. Chu, M. Zhang, W. Sun, F. Zhou, Association between neddylation and immune response, Front. Cell Dev. Biol. 10 (2022), https://doi.org/10.3389/fcell.2022.890121.
[63] C.A.B. Oliveira, E. Isaakova, P. Beli, D.P. Xirodimas, A Mass Spectrometry-Based Strategy for Mapping Modification Sites for the Ubiquitin-Like Modifier NEDD8, 2023, pp. 137–149, https://doi.org/10.1007/978-1-0716-2859-1_10.
[64] S. Lobato-Gil, J.B. Heidelberger, C. Maghames, A. Bailly, L. Brunello, M. S. Rodriguez, P. Beli, D.P. Xirodimas, Proteome-wide identification of NEDD8 modification sites reveals distinct proteomes for canonical and atypical NEDDylation, Cell Rep. 34 (2021) 108635, https://doi.org/10.1016/j.celrep.2020.108635.
[65] T. Sun, Z. Liu, Q. Yang, The role of ubiquitination and deubiquitination in cancer metabolism, Mol. Cancer 19 (2020) 146, https://doi.org/10.1186/s12943-020-01262-x.
[66] A. Hershko, A. Ciechanover, The ubiquitin system, Annu. Rev. Biochem. 67 (1998) 425–479, https://doi.org/10.1146/annurev.biochem.67.1.425.
[67] K. Hirota, Basic biology of hypoxic responses mediated by the transcription factor HIFs and its implication for medicine, Biomedicines 8 (2020) 32, https://doi.org/10.3390/biomedicines8020032.
[68] R. Raynes, L.C.D. Pomatto, K.J.A. Davies, Degradation of oxidized proteins by the proteasome: distinguishing between the 20S, 26S, and immunoproteasome proteolytic pathways, Mol. Aspects Med. 50 (2016) 41–55, https://doi.org/10.1016/j.mam.2016.05.001.
[69] G. Ben-Nissan, M. Sharon, Regulating the 20S proteasome ubiquitin-independent degradation pathway, Biomolecules 4 (2014) 862–884, https://doi.org/10.3390/biom4030862.
[70] X. Zhang, J. Zhou, A.F. Fernandes, J.R. Sparrow, P. Pereira, A. Taylor, F. Shang, The proteasome: a target of oxidative damage in cultured human retina pigment epithelial cells, Investigative Opthalmology & Visual Science 49 (2008) 3622, https://doi.org/10.1167/iovs.07-1559.
[71] H.K. Johnston-Carey, L.C.D. Pomatto, K.J.A. Davies, The immunoproteasome in oxidative stress, aging, and disease, Crit. Rev. Biochem. Mol. Biol. 51 (2016) 268–281, https://doi.org/10.3109/10409238.2016.1172554.
[72] Y. Mao, Structure, dynamics and function of the 26S proteasome, in: Macromolecular Protein Complexes III: Structure and Function. Subcellular Biochemistry, Springer, Cham, 2021, pp. 1–151, https://doi.org/10.1007/978-3-030-58971-4_1.
[73] I. Sahu, S.M. Mali, P. Sulkshane, C. Xu, A. Rozenberg, R. Morag, M.P. Sahoo, S. K. Singh, Z. Ding, Y. Wang, S. Day, Y. Cong, O. Kleifeld, A. Brik, M.H. Glickman, The 20S as a stand-alone proteasome in cells can degrade the ubiquitin tag, Nat. Commun. 12 (2021) 6173, https://doi.org/10.1038/s41467-021-26427-0.
[74] J.-H. Ryu, S.-H. Li, H.-S. Park, J.-W. Park, B. Lee, Y.-S. Chun, Hypoxia-inducible factor α subunit stabilization by NEDD8 conjugation is reactive oxygen species-dependent, J. Biol. Chem. 286 (2011) 6963–6970, https://doi.org/10.1074/jbc.M110.188706.
[75] M.R. Littner, Mild obstructive sleep apnea syndrome should not be treated, J. Clin. Sleep Med. 3 (2007) 263–264. https://www.ncbi.nlm.nih.gov/pmc/articles/PMC2564770/ (accessed April 4, 2024).
[76] A. Castrogiovanni, M.R. Bonsignore, May continuous positive airway pressure (CPAP) treatment be detrimental in obstructive sleep apnea? EBioMedicine 101 (2024) 105052 https://doi.org/10.1016/j.ebiom.2024.105052.